



**POLITECNICO**  
MILANO 1863

SCUOLA DI INGEGNERIA INDUSTRIALE  
E DELL'INFORMAZIONE

# Pd-Loaded Nanocellulose-Based Materials as Heterogeneous Catalysts for Suzuki-Miyaura Coupling Reactions

TESI DI LAUREA MAGISTRALE IN:  
MATERIALS ENGINEERING AND NANOTECHNOLOGY  
INGEGNERIA DEI MATERIALI E DELLE NANOTECNOLOGIE

**Author: Liu Mingchong**

Student ID : 939753

advisor: Prof. Carlo Punta

Co-advisor: Prof. Alessandro Sacchetti, Dr. Laura Riva

Academic Year: 2021-2022



## Abstract

Among materials of natural origin and bio-friendly, cellulose turns out to be very versatile and easy to functionalize, combining high reactivity and eco-compatibility. In this study, TEMPO-oxidized cellulose nanofibers and cross-linking agents (branched polyethyleneimine and citric acid) were combined to form nanosponges based on nanocellulose with cross-linked structure that were used as support for Palladium, obtaining a novel heterogeneous catalyst for Suzuki-Miyaura coupling reactions. The microstructure and Pd loading on CNS were investigated by scanning electron microscopy (SEM) analysis with energy-dispersive X-ray spectroscopy (EDS) detector and by inductively coupled plasma-optical emission spectrometry (ICP-OES) analysis. The resulting materials show high efficiency as heterogeneous catalysts for promoting the Suzuki-Miyaura reaction. With the help of a microwave reactor, several reaction parameters were studied: reaction time, temperature, amount of phase transfer catalyst and percentage of catalyst.

The optimized conditions allow the reaction to get more than 97% yield. Reusability tests of this cellulose-based Pd loaded catalyst were also conducted, showing catalytic activity up to 4 reuses. The high cost of Palladium and sustainable development of new technologies were considered for these tests.

**Keywords:** TEMPO-oxidized cellulose nanofibers, cellulose nanosponges, Suzuki-Miyaura coupling, palladium catalyst



## Abstract in lingua italiana

Nell'ultimo decennio l'Unione Europea si sta muovendo sempre più verso una transizione verde e tematiche come la conservazione dell'energia, la riduzione delle emissioni di carbonio, la chimica verde e lo sviluppo sostenibile dell'industria chimica stanno diventando sempre più importanti. In questo contesto si inserisce perfettamente la cellulosa, che tra i materiali di origine naturale e bio-friendly risulta essere molto versatile e facile da funzionalizzare, combinando alta reattività ed eco-compatibilità. In questo studio, nanofibre di cellulosa TEMPO-ossidate e agenti reticolanti (polietilenimina ramificata e acido citrico) sono stati combinati per formare nanospugne a base di nanocellulosa con struttura reticolata che sono state utilizzate come supporto per il Palladio, ottenendo un catalizzatore eterogeneo innovativo per le reazioni di accoppiamento Suzuki-Miyaura. La struttura morfologica e il caricamento del metallo su queste nanospugne sono stati studiati con metodi analitici SEM-EDS e ICP-OES. I materiali ottenuti come catalizzatori eterogenei hanno mostrato un'alta efficienza nel promuovere le reazioni di accoppiamento Suzuki-Miyaura.

Con l'aiuto di un reattore a microonde, sono stati studiati diversi parametri di reazione: tempo di reazione, temperatura, quantità di catalizzatore di trasferimento di fase e percentuale di catalizzatore. Nelle condizioni ottimali è stata ottenuta una resa di reazione superiore al 97%.



Sono stati anche condotti test di riutilizzo di questo catalizzatore caricato con Pd a base di cellulosa, mostrando attività catalitica sino a 4 riutilizzi. Per questi test gli alti costi del Palladio e lo sviluppo sostenibile di nuove tecnologie sono stati presi in considerazione.

**Parole chiave:** nanofibre di cellulosa ossidate TEMPO, nanospugne di cellulosa, accoppiamento Suzuki-Miyaura, Catalizzatore al Palladio





# Contents

<b>Abstract.....</b>	<b>i</b>
<b>Abstract in lingua italiana .....</b>	<b>iii</b>
<b>Contents .....</b>	<b>vii</b>
<b>1. Introduction .....</b>	<b>1</b>
1.1 Green chemistry and Sustainability .....	1
1.2 Cellulose.....	5
1.2.1 Overview of cellulose .....	5
1.2.2 Nanocellulose.....	7
1.2.3 Nanocellulose.....	8
1.2.4 Cellulose Nano-sponge(CNS).....	11
1.3 Suzuki-Miyaura coupling.....	14
1.3.1 General overview .....	14
1.3.2 Catalysts and Heterogeneous Catalysis .....	17
<b>2. Materials and Methods .....</b>	<b>22</b>
2.1 Materials preparation.....	22
2.1.1 Preparation of TEMPO-Oxidized Cellulose(TOC) .....	23
2.1.2 Titration of TOC .....	23
2.1.3 Preparation of cellulose nanosponges(CNS) .....	24
2.1.4 Preparation of heterogeneous catalyst CNS-Pd.....	25
2.2 Characterization.....	26
2.2.1 SEM and EDS Analysis.....	26
2.2.2 ICP-OES and Leaching test .....	26
2.3 Suzuki-Miyaura coupling.....	28
2.3.1 Basic standard reaction.....	28
2.3.2 Reaction treatment and product purification.....	28

2.3.3	Condition optimization .....	30
2.3.4	Recycling and Reuse .....	30
2.3.5	Scope of reaction.....	30
<b>3.</b>	<b>Result and Discussion.....</b>	<b>33</b>
3.1	Materials and Products .....	33
3.2	Materials characterization .....	37
3.2.1	SEM and EDS analysis.....	37
3.2.2	ICP-OES and Leaching test .....	40
3.3	Yield and conversion.....	42
3.4	Optimization condition.....	43
3.4.1	Time and Temperature .....	43
3.4.2	Catalyst, Base and TBAB .....	45
3.4.3	Amplify the reaction .....	48
3.4.4	Recycling and reuse .....	49
3.4.5	Scope of reaction.....	50
<b>4.</b>	<b>Conclusion and Outlook .....</b>	<b>52</b>
<b>5.</b>	<b>Bibliography .....</b>	<b>54</b>
<b>A.</b>	<b>Appendix A .....</b>	<b>59</b>
	<b>List of Figures.....</b>	<b>65</b>
	<b>List of Tables.....</b>	<b>67</b>
	<b>Acknowledgements .....</b>	<b>69</b>

# 1. Introduction

## 1.1 Green chemistry and Sustainability

In the 1990s, after more than 30 “silent springs”, mankind finally began to face up to the environmental pollution caused by the chemical industry. The concepts of "sustainable development" and "green chemistry" were born<sup>[1]</sup> rapidly, and were quickly incorporated into major development strategies by most countries around the world. Led by the government, green chemistry embarked on the road of development. From concept to realization, there is a long way to go. The governments of many countries have cooperated with industry-university-research circles to gradually establish the 12 principles of green chemistry, atomic economy, and the 5Rs(Reduce, reuse, recycle, regeneration, rejection) of green chemistry<sup>[1]</sup>. As the second largest chemical production and consumption area in the world<sup>[2]</sup>, the EU carries the mission of practicing green chemistry.

For this purpose, green technology has entered the budding stage. Academia and industry work together as the main force to explore green chemistry technology based on multiple application fields<sup>[1]</sup>.

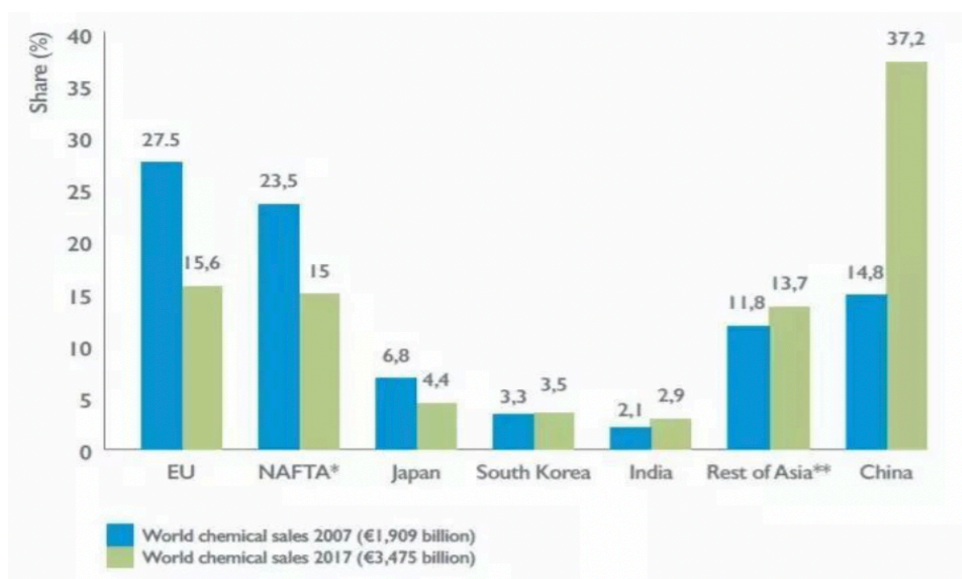


Figure 1. World chemical sales by region in 2017

On December 11, 2019, the European Commission issued a new growth strategy document, the European Green Deal (hereinafter referred to as the "New Deal"). The draft of the New Deal proposes to make Europe the world's first carbon-neutral continent by 2050 through the transition to clean energy and a circular economy, in order to prevent climate change and promote the stable and sustainable development of the European economy. The draft of New Deal not only proposes the EU's 2050 carbon neutrality target, but also proposes a policy roadmap for implementing the target, which will have a profound impact on the EU's economic and social development. Among them, the requirements of the industrial system, especially the chemical industry system, have raised a lot of challenges, requiring the chemical industry in the EU to strictly abide by the concept of green chemistry and achieve a sustainable low-carbon chemical industry.

At the same time, we can see that on March 15, 2021 the EU approved a new chemicals strategy that sets a long-term vision for EU chemicals policy. The Council believes that

the strategy aims to achieve a non-toxic environment with a higher level of protection for human health and the environment, while enhancing the competitiveness of the EU chemical industry. In this conclusion, the Council asked the Commission to implement the actions set out in the strategy, including targeted amendments to streamline EU chemicals legislation, replace and reduce substances of concern, and phase out chemicals most harmful to non-essential social uses.

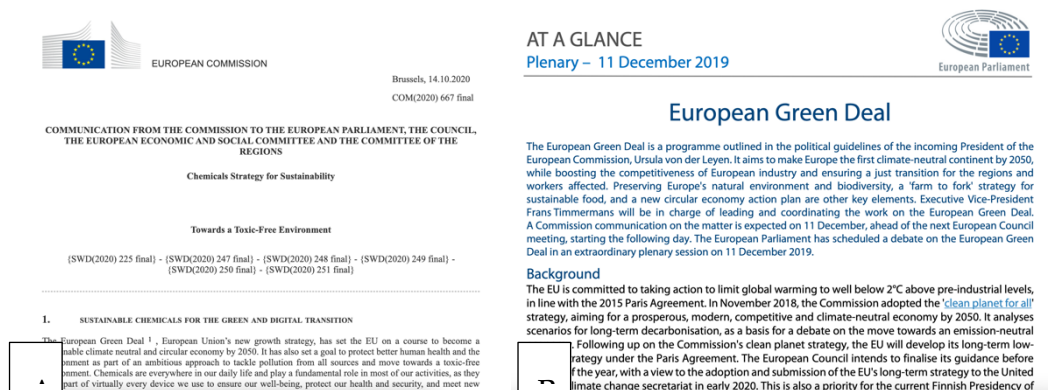


Figure 2. A: new chemicals strategy that sets a long-term vision for EU chemicals policy; B: European Green Deal

From the perspective of technology chain, the source innovation technologies of green chemistry are clustered into four categories - catalytic systems, reactions and processes, green products and photo electrochemistry. The four types of technologies have been diffused and integrated to form a green chemical technology network. At present, many technologies have been extended to application fields, from technical research to technical services. The main service fields are green reaction, green products, clean synthesis process, renewable resource conversion, new energy utilization and pollutant waste treatment. The catalytic system has been continuously improved and perfected, from traditional chemical catalysis to three powerful means: chemical, biological and combined catalysis. Among them, chemical catalysis aims to improve

the efficiency of catalysts, expand the scope of substrate application and reduce the cost of use<sup>[5]</sup>.

## 1.2 Cellulose

### 1.2.1 Overview of cellulose

Cellulose is the most abundant and renewable natural organic polymer in nature<sup>[28]</sup>, and its sources are very wide, including plants, marine organisms<sup>[29]</sup> and microorganisms<sup>[28]</sup>. The chemical structure of cellulose is a macromolecule composed of glucopyranose units connected by  $\beta$ -1,4-glycosidic bonds. Each glucose unit has hydroxyl groups on C2, C3, and C6. Hydrogen bonds may form between them, so cellulose molecules may form crystalline structures<sup>[30]</sup>. In nature, the cellulose content of cotton is the highest, reaching more than 90%, wood is 40% to 50%. In addition, hemp, straw, wheat straw, bamboo etc. are also rich in cellulose<sup>[28]</sup>. As we all know, cellulose-containing plant fiber is the basic raw material for paper production. but cellulose extracted from cotton or plant fiber is also an important chemical raw material, which has wide application value in the fields of textiles, clothing, medicine and health, building materials and coatings<sup>[30]</sup>

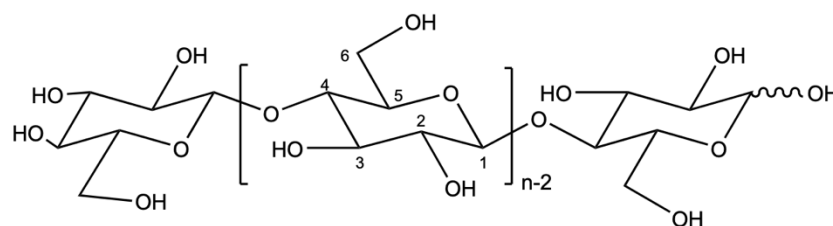
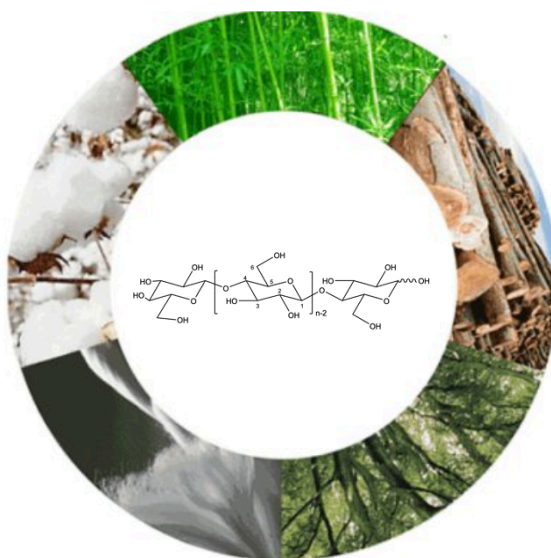


Figure 3. Cellulose molecular structure

As one of the most important structural elements in plants and some bacteria, the main function of cellulose is to provide support for cells and bodies. This gives it many desirable properties, including low density, non-toxicity, and high biodegradability<sup>[31]</sup>. Almost pure cellulose can be found in cotton fibers, while in wood, plant leaves and

stems it is combined with other materials, namely lignin and hemicellulose [32]. The underlying determinants of the mechanical and chemical properties of cellulose are the length of the segments and the treatment used to obtain the cellulose. This means that cotton, plant fibers and bacteria provide longer chains than wood[33]. It is generally accepted that cellulose is an almost inexhaustible biomaterial, accounting for approximately  $1.5 \times 10^{12}$  tons of annual biomass production[33]. But what we cannot ignore is that a large amount of cellulose is also treated as waste every year, and most of the sources of these waste cellulose come from single consumables in daily life, such as used paper, construction wood, agricultural residues and food waste[31]. Recycling and reusing these "waste" celluloses is one of the current mainstream low-carbon economic directions for the purpose of high-efficiency chemistry[34].



*Figure 4. Variety of cellulose sources*



### 1.2.2 Nanocellulose

In recent years, with the deepening and development of nanotechnology in the field of pulping, papermaking and materials, the development of nanomaterials from biomass cellulose and the preparation of functional materials using its special properties have gradually attracted researchers' attention. Among them, nanocellulose is represented by a series of physical or chemical properties, namely nano-dimension, superior mechanical properties (elastic modulus is about 150 GPa), high specific surface area, high aspect ratio, high reactivity, low thermal expansion coefficient, renewable, biodegradable, good biocompatibility etc.<sup>[45]</sup> All these properties make nanocellulose a functional polymer material with broad application prospects. At present, nanocellulose has been successfully applied in nano-functional materials, such as aerogels<sup>[46][47]</sup>, biomedical materials<sup>[48][49]</sup>, food packaging materials <sup>[50][51]</sup>, nanocomposite materials<sup>[52][53]</sup>, optoelectronic materials etc, which greatly improve the added value and utilization efficiency of biomass cellulose. Depending on the size, morphology and preparation method, nanocellulose can be categorized as follow: Cellulose Nanocrystals (CNC), Cellulose Nanofibrils (CNF), Bacterial Cellulose (BNC), Electro-spun Cellulose Nanofibrils (ECNF).

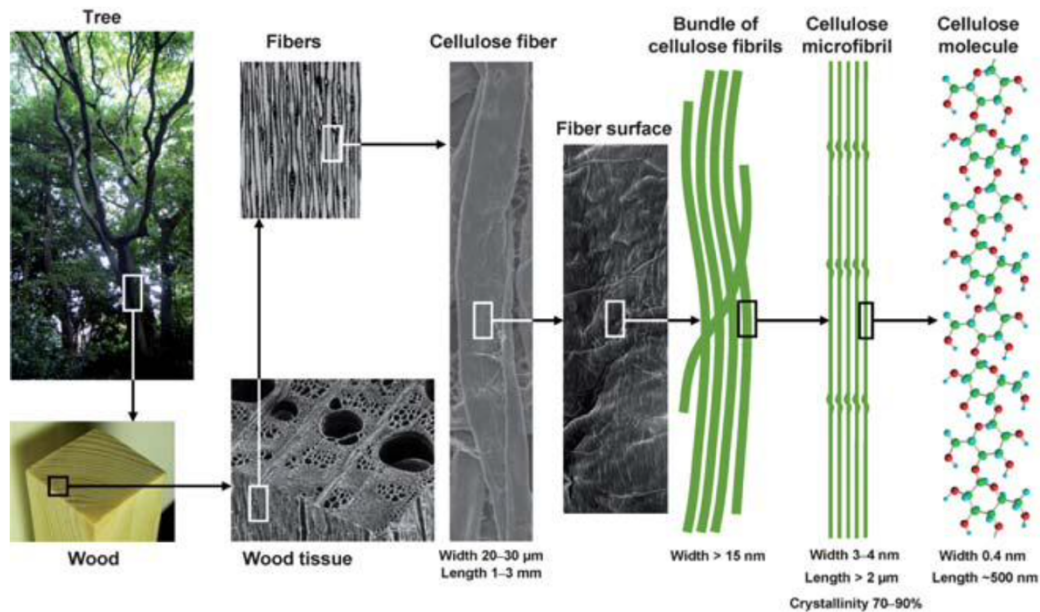


Figure 5. Cellulose hierarchical architecture

### 1.2.3 Nanocellulose

In view of the so many advantages of cellulose nano-fiber, more modification and research has been focused on it and make it more widely concerned. Compared with cellulose nanofibers prepared by other methods, TOCNFs (TEMPO-Oxidized cellulose nano-fibers) have the advantages of high crystallinity, uniform width, large aspect ratio, so they are superior in composite applications<sup>[36]</sup>.

TEMPO catalyzes the oxidation of cellulose C6-hydroxyl groups to C6-carboxyl groups as shown in Figure 6<sup>[35]</sup>. NaClO is the main oxidant in this process. It first forms NaBrO with NaBr, and then NaBrO oxidizes TEMPO to nitronium ion, which oxidizes primary alcohol hydroxyl group to aldehyde group (intermediate), and finally generates carboxyl group<sup>[37]</sup>. With the study of this system, scholars have found that

the reaction under alkaline conditions will cause violent depolymerization of cellulose molecules<sup>[39][40]</sup>, and the degree of polymerization affects the strength and flexibility of cellulose fibers, which is related to its prosperities in applications and final performance<sup>[41]</sup>. Therefore, in order to maintain the properties of cellulose fibers, it should be oxidized in neutral or weak acid. Oxidation mechanism is reported in Figure 6 and 7<sup>[43]</sup>. The two systems to oxidase cellulose are showed in the following:

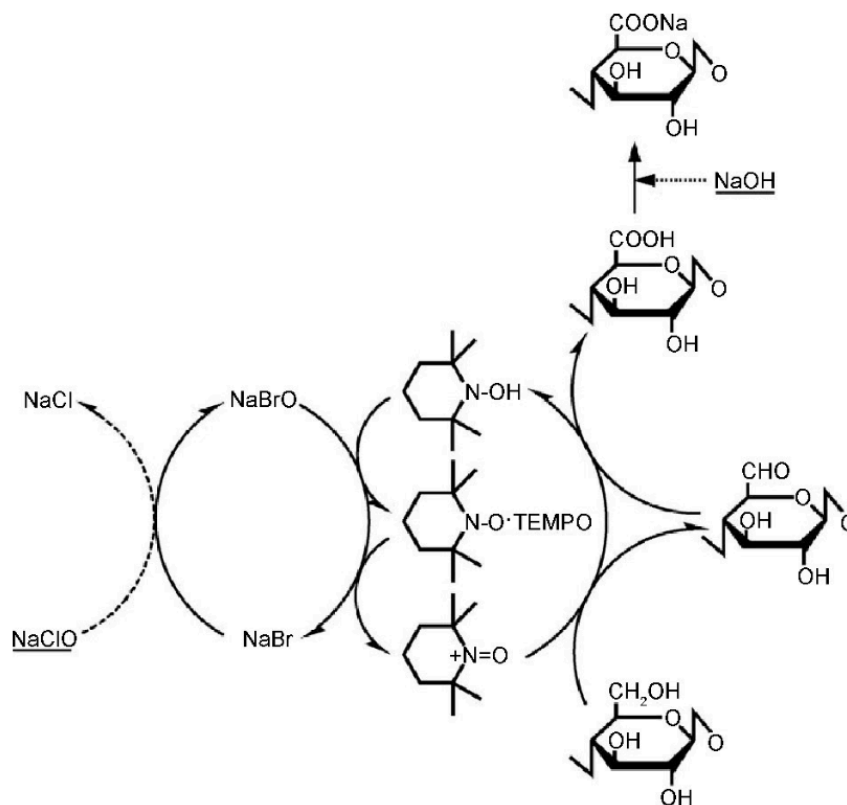


Figure 6. TEMPO-mediated oxidation of cellulose to form C6-carboxylate groups via C6-aldehyde groups

TEMPO catalyzes the oxidation of cellulose C6-aldehyde groups to C6-carboxyl groups as shown in Figure 6. NaClO is the main oxidant in this process, which first forms NaBrO with NaBr, and then NaBrO oxidizes TEMPO to nitrosonium ion, which oxidizes primary alcohol hydroxyl group to aldehyde group (intermediate), and finally generates Carboxyl. With the study of this system, researchers have found that the reaction under alkaline conditions will cause the cellulose molecules to decompose violently<sup>[40]</sup>, and the degree of cellulose polymerization affects the strength and flexibility of its fibers, which is directly related to its performance in applications. Therefore, in order to maintain the properties of cellulose fibers, the cellulose should be oxidized under neutral or weak acidity. In addition, some aldehyde groups remain in the oxidized cellulose by the TEMPO/NaBr/NaClO system. The thermal instability of the aldehyde groups will cause the oxidized cellulose to change color when the heating or drying temperature exceeds 80 °C<sup>[40]</sup> <sup>[41]</sup>, and the residual aldehyde groups will also form between fibers. Hemiacetal bonds affect fiber dispersion. With further studies, the researchers found that the TEMPO/NaClO/NaClO<sub>2</sub> system can overcome the defects of the TEMPO/NaBr/NaClO system, using NaClO<sub>2</sub> as the main oxidant, and the reaction mechanism is shown in Figure 7

Saito et al. <sup>[43]</sup> treated hardwood pulp with TEMPO/NaClO/NaClO<sub>2</sub> system, the oxidized cellulose carboxyl group content was 0.8 mmol/g without aldehyde groups, and the cellulose nanofibers obtained by homogenization treatment had a width of 5 nm and a length of 5 nm. In addition, the addition of a small amount of NaClO (1.0 mmol/g cellulose) is also very important for the oxidation of cellulose in this system, because the addition of NaClO can accelerate the oxidation reaction<sup>[43]</sup>. However, the TEMPO/NaClO/NaClO<sub>2</sub> system has disadvantages such as long reaction time and

relatively low carboxyl group content. So people can choose the acceptable condition for oxidation based on their need.

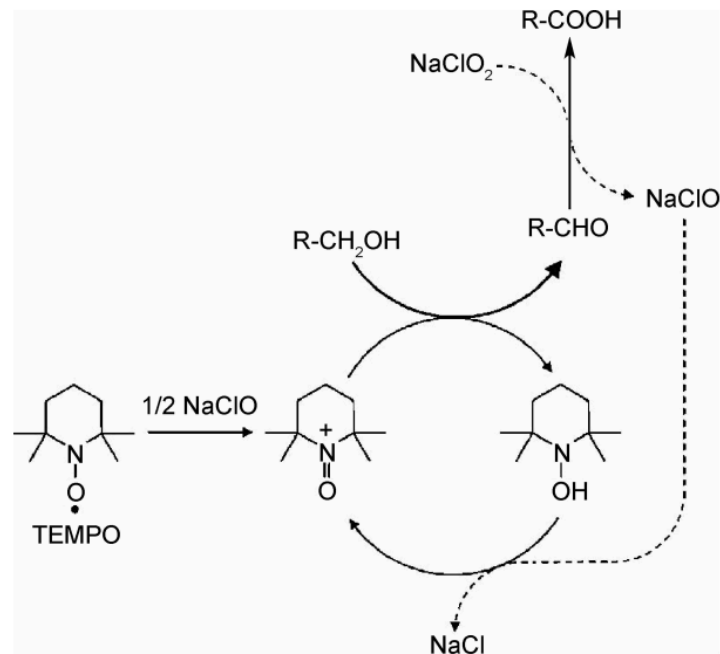


Figure 7. Oxidation of primary hydroxyls to carboxyl groups by the TEMPO/NaClO/NaClO<sub>2</sub> system under weakly acidic or neutral condition

#### 1.2.4 Cellulose Nano-sponge (CNS)

In 2015, Melone et al. reported the synthesis of cellulose nanosponges (CNS)<sup>[54]</sup>, a new porous bio-based nanomaterial obtained from TEMPO-oxidized cellulose. These CNS greatly broadened the application range of cellulose-based new materials. They are thermally prepared to facilitate cross-linking between TEMPO oxidized cellulose nanofibers (TOCNF) and branched polyethyleneimine (bPEI). The cross-linking is based on the formation of amides between the carboxyl groups of TOCNF and the primary amino groups mainly present in bPEI<sup>[55]</sup>.

The development of this first solution led to the introduction of citric acid (CA) as a co-crosslinking agent<sup>[56]</sup>, providing an additional source of carboxylic groups. As an auxiliary agent, CA can fix bPEI in the cellulose grid, improving the degree of cross-linking, and reducing the amount of bPEI. CNS are characterized by a high micro- and nano-porosity, as demonstrated by previous works<sup>[58]</sup>. This porosity is the result of the freeze-drying process during the CNS preparation, in which ice crystals behave as templates for pores formation and are then removed by sublimation<sup>[59]</sup>. The structure of CNS materials is highly porous, which provides a large exposed superficial area. Thanks to the interaction of organic molecules with the porous architecture of CNS, compared to TOCNF, CNS clearly show superior sorption capacity. The main application directions include water purification and water remediation<sup>[54][57]</sup>, no matter be used for inorganic and organic contaminants. The amino groups, from the bPEI part, are able to effectively chelate heavy metal ions, imparting superb adsorption capacity to the CNS, both in freshwater and in seawater. While at the same time, according to the recent work at O<sup>SCM</sup> Lab<sup>[61]</sup>, the biomass materials can be used as metal carriers for heterogeneous catalysis in organic chemistry. In the work at O<sup>SCM</sup> lab, the moderately sized CNS voids can allow multiple metal ions to be loaded thanks to the chelating action of the amino groups from bPEI. The group prepared a CNS-Cu and CNS- Zn, which provides the possibility to achieve heterogeneous catalysis.<sup>[61]</sup>

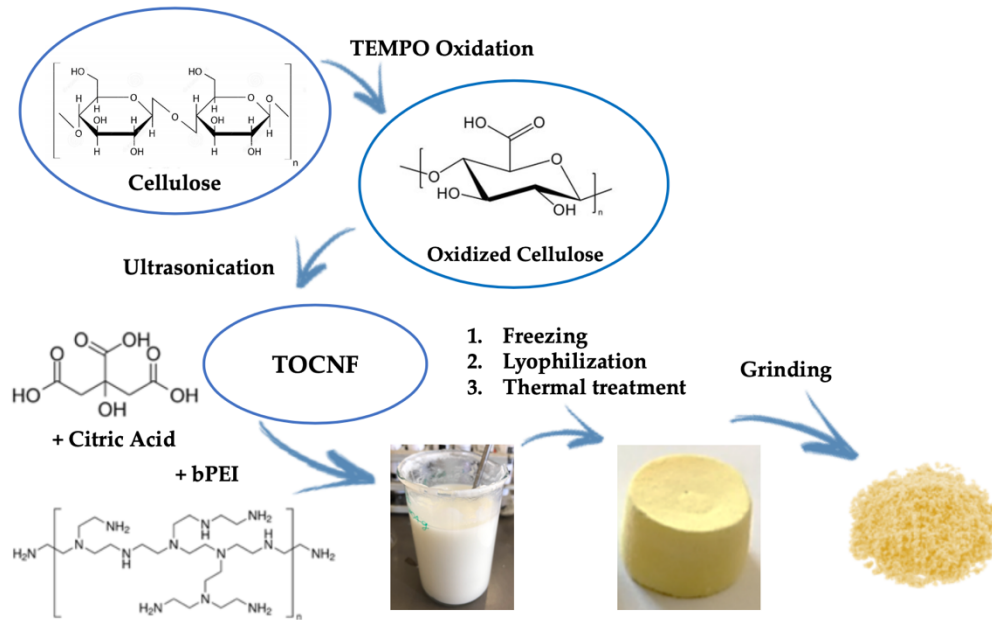


Figure 8. Production scheme of cellulose nanosponges (CNS)

## 1.3 Suzuki-Miyaura coupling

### 1.3.1 General overview

In the past four decades, the frequency of chemical reactions used by medicinal chemists to construct carbon-carbon bonds has shown a very significant upward trend, and the wide application of carbon-carbon bond construction and the discovery of Suzuki-Miyaura coupling (Suzuki reaction or Suzuki coupling) reactions are closely related to In 1979, Suzuki and Miyaura<sup>[7]</sup> first reported the coupling reaction of transition metal palladium-catalyzed organoboronic compounds and halogenated hydrocarbons under the action of bases. Subsequently, the two of them developed this coupling method. The palladium-catalyzed reaction of organoboronic compounds with (similar)halides is called the Suzuki-Miyaura coupling reaction. It has the outstanding advantages of wide universality, stable and low toxicity of organoboronic compounds reagents and a wide range of sources<sup>[7]</sup> whether it is in fine chemicals<sup>[9]</sup>, medicines<sup>[1][9]</sup>, pesticides<sup>[10]</sup> and organic materials<sup>[12]</sup>, it has a wide range of applications from the laboratory milligrams scale to the industrial scale of hundreds of kilograms<sup>[13]</sup>.

The catalytic cycle of the Suzuki-Miyaura coupling reaction is generally divided into three basic steps: (1) insertion of zerovalent palladium into carbon-halogen bond to form divalent palladium—oxidative addition; (2) oxidative addition of organoboron reagents where the nucleophilic group migrates to palladium—transmetalation; (3) Simultaneous generation of coupling product and zero-valent palladium (zero-valent palladium will undergo subsequent oxidative addition to complete the next catalytic cycle)—reductive elimination. Compared with the extensiveness of the Suzuki-Miyaura coupling reaction, the mechanism study of the Suzuki-Miyaura coupling



reaction is relatively lagging behind. At present, people have a relatively clear understanding of the oxidative addition and reductive elimination processes, but still lack sufficient understanding of the transmetalation process. The actual Suzuki-Miyaura coupling reaction is affected by a variety of factors, and the three steps of oxidative addition, transmetalation and reductive elimination can also present different reaction paths under the influence of different factors.

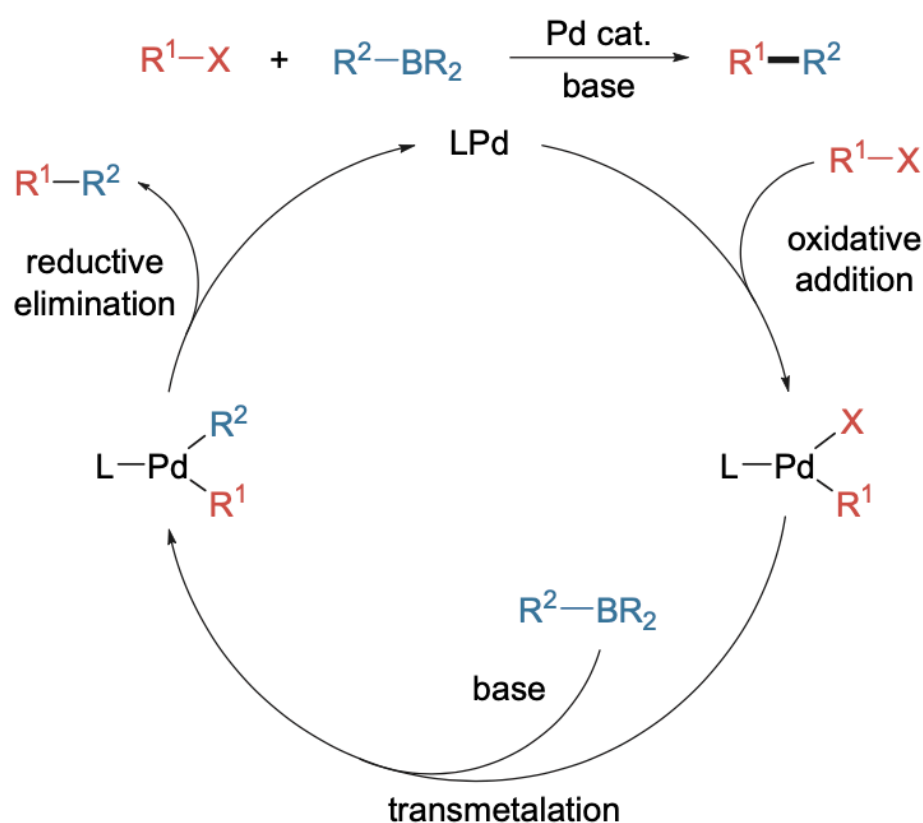


Figure 9. Basic mechanism scheme of Suzuki-Miyaura coupling

Oxidative addition generally means that the valence state of the central metal increases by two during the reaction process, accompanied by the increase of two coordinating groups. Transmetalation generally refers to the transfer of the ligand connected to the

metal center to another a metal-centered process. Boron is a special metalloid element, and the organic group connected to the boron atom in organoborides has strong nucleophilicity, so it is similar in chemical reactivity to metal-organic reagents. For the Suzuki-Miyaura reaction, transmetalation is the process in which the organic group of the organoboron reagent is transferred from the boron atom to the transition metal palladium. The reduction and elimination can be regarded as the reverse process of oxidative addition. During the reaction, the covalent bond coupling with two ligands coordinated by palladium reduces the valence of palladium at the same time. The reduction and elimination process of the Suzuki-Miyaura coupling reaction starts from the transmetalation intermediate, and the C-C bond coupling product is obtained after the reaction.

In more than 40 years since the discovery of the Suzuki coupling reaction, researchers have developed a variety of Suzuki-Miyaura reaction types, greatly enriching and expanding the Suzuki-Miyaura reaction.

Palladium is a precious metal, and its cost problem in large-scale synthesis is highlighted. After continuous exploration, researchers have developed the Suzuki-Miyaura coupling reaction involving catalysts such as nickel, copper, cobalt, iron and cobalt<sup>[14]</sup>. In addition, the transition metal-free Suzuki-Miyaura coupling reaction was recently realized. In 2018, Huang Yong and his collaborators<sup>[15]</sup> reported the non-transition metal-catalyzed Suzuki-Miyaura reaction.

Suzuki-Miyaura coupling reactions generally use organic halides as electrophiles. With the continuous development of Suzuki-Miyaura coupling reactions, more and more types of electrophiles are compatible with organoboron coupling reactions. The base-free Suzuki-Miyaura coupling can further expand the substrate range and is

compatible with base-sensitive substrates. In 2013, Ogoshi and his collaborators<sup>[16]</sup> developed a base-free perfluoro ethylene and aryl Method for boronated coupling. In 2017, Carrow and collaborators<sup>[17]</sup> developed another strategy to achieve base-free Suzuki-Miyaura coupling.

### 1.3.2 Catalysts and Heterogeneous Catalysis

Homogeneous catalytic systems are very attractive in industrial catalysis because all reactants, reagents and catalysts are dissolved in the same reaction medium, which is beneficial to expand the reaction range and to large-scale production. Compare the advantages such as high activity and high selectivity, limited thermal stability is one negative factor that makes it is hard to remove homogeneous catalysts from the reaction mixture.

Different with the previous homogeneous catalysts, the heterogeneous ones are easy to separate from the reaction mixture and have good recyclability, so they are widely used in synthetic chemistry. New metal catalysts usually supported on carbon, magnetic materials, silica, inorganic oxides, zeolites, functionalized nanomaterials, metal-organic frameworks (MOFs), organic polymers, clay minerals, biomass material and the surface of insoluble solid supports such as bio-supports<sup>[19]</sup>. That composites help to overcome the difficult separation and carryover of homogeneous catalysts contamination and other disadvantages. However, most heterogeneous catalysts are not highly selective, but can rely on metal loading to tune the reaction, ultimately avoiding product contamination and making separation easy<sup>[19]</sup>.

In recent years, due to the better performance and cost-effectiveness of metal nanoparticles, there has been increasing interest in their application as catalysts.

Researchers have been working to control the surface properties and chemical activity of metal nanoparticles. Since Nanoparticles are small in size and large in surface area<sup>[20][21]</sup>, so they have higher reactivity than specific metal nanoparticles. Therefore, most of the active metals in heterogeneous catalysts exist in the form of nanoparticle.

### **Different catalyst supports**

In one aspect, nano-palladium catalysts supported by ionic liquids (ILs) have been widely used, as this method allows us to simultaneously achieve avoidance of highly toxic solvents and efficient catalyst recycling. Nacci's group<sup>[20]</sup> has proposed that tetra-alkylamine-based ionic liquids, palladium nanoparticles can be used as catalysts for the Suzuki coupling reaction of aryl halides.

SiO<sub>2</sub> is widely used as support for heterogeneous catalysis due to the high efficiency, stability, high specific surface area, and recyclability. SiO<sub>2</sub>-based materials contain silanol groups, which can be loaded after functionalization with different transition metals. In 2013, Speziali et al.<sup>[22]</sup> studied a heterogeneous catalytic system using MCM-41 and SiO<sub>2</sub> as supports to support palladium and palladium-gold nanoparticles, and successfully applied the nano-catalysts in the presence of KOH, Ligand-free Suzuki coupling reaction in water at 80 °C.

Magnetic nanoparticles have attracted great interest due to the low toxicity, high specific surface area, superparamagnetic properties, and easily magnetization. They are removed from the reaction mixture by an external magnetic field, and thus, magnetic nanoparticles are one of the new choices for the preparation of recyclable heterogeneous. Waghmode et al.<sup>[23]</sup> made another important discovery in the field of heterogeneous palladium catalysts by using surface-modified  $\text{NiFe}_2\text{O}_4$  as a catalyst support for palladium nanoparticles. That materials can show magnetism undergo the external magnetic field

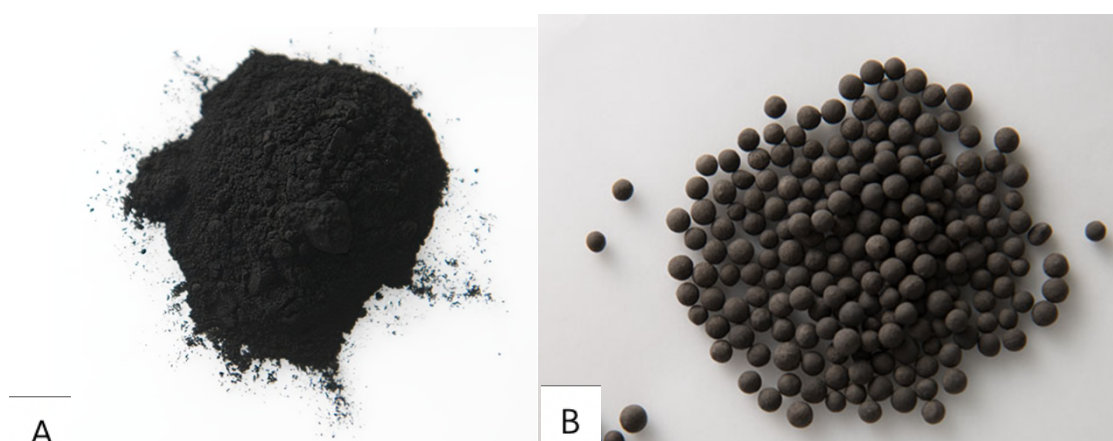


Figure 10. Different Pd catalysts, A: Pd/C; B: Pd/Al<sub>2</sub>O<sub>3</sub>

The use of solid-supported catalysts offers the advantages of easy recovery and recyclability, thus providing a sustainable and low-cost fabrication platform.

Palladium-carbon (Pd/C) catalysts are not only widely used in various types of hydrogenation catalyst reactions. It is widely used in cross-coupling reactions<sup>[24]</sup>. Liu et al.<sup>[25]</sup> reported a condition of no ligand, with Pd/C (3% (mol%)) as the catalyst, with the mixture of water and ethanol as the solvent, the base is  $\text{K}_2\text{CO}_3$ , the aryl bromide is coupled with the aryl boronic acid in the air at room temperature.

Natural biopolymers such as chitosan, cellulose, and wool have been effectively used in many palladium-catalyzed organic reactions. Most of these require further modification at appropriate inner diameter, degree of polymerization, and cross-linking. In 2011, Firouzabadi<sup>[26]</sup> used agarose hydrogels as carriers for palladium nanoparticles and bio-organic ligands, which has been effectively applied in the Suzuki coupling reaction in water. Lei et al.<sup>[40]</sup> studied natural animal fibers (wool) as a carrier, which did not require any modification, but supported uniformly distributed nano-palladium on the fiber surface. The advantages of this catalyst are: (1) No additional modification required; (2) Reaction in water under air conditions; (3) Heterogeneous catalysts are insoluble in water; (4) High stability, easy separation and recyclability powerful



## 2. Materials and Methods

### 2.1 Materials preparation

All of the reagents were purchased from Merck. Cotton linter was obtained from Bartoli paper factory (Capannori, Lucca, Italy). Deionized water was produced within the laboratories with a Millipore Elix® Deionizer with Progard® S2 ion exchange resins. The solvents such as ethyl acetate, n-hexane and ethanol required for the treatment reaction are all analytically pure solvents used in the laboratory experiments and purchased from Carlo Erba. All <sup>1</sup>H-NMR spectra were recorded on a 400 MHz Brüker <sup>1</sup>H-NMR spectrometer. Microwave reactions were conducted in a Biotage® Initiator+. Other equipment used in the procedures include a Branson SFX250 Sonicator, a SP Scientific BenchTop Pro Lyophilizer, a Büchi Rotavapor® R-124 8 and a Thermotest—Mazzali laboratory oven. Scanning electron microscopy (SEM) was performed using a variable pressure instrument (SEM Cambridge Stereoscan 360) at 100/120 pA with a detector BSD. The operating voltage was 15 kV with an electron beam current intensity of 100 pA. The focal distance was 9 mm. The EDS analysis was performed using a Bruker Quantax 200 6/30 instrument. The metal concentrations were measured by ICP-OES atomic emission spectroscopy using a Perkin Elmer Optima 3000 SD spectrometer



### 2.1.1 Preparation of TEMPO-Oxidized Cellulose Nanofibers (TOCNF)

For the preparation of TEMPO-Oxidized cellulose nanofibers (TOCNF), 20 g of cotton linters were cut and chopped with the help of a home mini blender in 350 mL of deionized water, after which the reaction batch was placed on a magnetic stirrer. Meanwhile, 0.43 g of TEMPO and 3.082 g of KBr were dissolved in 250 mL of deionized water at room temperature with the aid of magnetic stirring until complete dissolution. Then, chopped cotton linters was added to the solution. 87.4 mL of 12% w/v NaClO solution in deionized water were gradually dropped into the mixture and then a few drops of 4 M aqueous NaOH were added until the pH reached a stable value between 10.5 and 11.00, indicating that the oxidation process has reached a plateau. After stirring for 16 h at room temperature, 4-6 mL of 12 M HCl solution were added to reduce the pH to a value between 1 and 2, resulting in the aggregation of the fibers. Finally, the mixture was washed with deionized water to neutral pH and filtered through a Büchner funnel connected to a vacuum pump. The obtained material was dried in air at room temperature for 48 h. The final yield of the process was calculated to be 76.5% (15.37 g of dry TOC).

### 2.1.2 Titration of TOC

The titration process aims to determine the degree of oxidation of TOC in the previous step. The degree of oxidation refers to the amount of carboxyl groups in each gram of material, in units of mmol/g. This step requires the use of 0.1 N titrated and NaOH solution, and the colorimetric indicator used in the titration process is phenolphthalein. The titration was performed by dispersing 514 mg of dried TOC in deionized water with the aid of a ultrasonicator, obtaining TEMPO-Oxidized Cellulose Nanofibers (TOCNF) and ensuring that the mixture was relatively homogeneous. After adding 3-4 drops of phenolphthalein, the sonication operation was repeated to help the

dispersion of the indicator and to optimize the titration process for reaching high accuracy. Then, the previously titrated NaOH 0.1 N solution was put into a burette and dropped it into the dispersion until the stable pink color of the suspension could be observed, which means that the equivalent point was reached, and the NaOH 0.1 N solution used for the titration was recorded to be 6.6 ml. Finally, the oxidation degree of TOC was calculated as reported in **Equation 1**:

$$\text{Oxidation degree} = \frac{0.1031 \cdot 6.5}{0.514} = 1,304 \frac{\text{mmol}_{\text{COOH}}}{\text{g}_{\text{TOCNF}}} \quad [1]$$

### 2.1.3 Preparation of cellulose nanospheres(CNS)

For the preparation of CNS, 5 g of dry TOC were dispersed in 250 mL of deionized water to prepare a 2% w/v dispersion. Solid NaOH was then added to the suspension and the amount was calculated by means of **Equation 2** and **3**:

$$\text{Total mmol of COOH groups} = 1.31 \frac{\text{mmol}}{\text{g}} * 5 \text{ g} = 6,55 \text{ mmol} \quad [2]$$

$$\text{Amount of NaOH} = 6,55 \text{ mmol} \times 40 \text{ mg/mmol} = 262 \text{ mg} \quad [3]$$

After the complete dispersion of TOC with the aid of an ultrasonicator (5 min), 10 ml of 0.5M HCl solution were added to induce fiber coagulation. After a clear morphological change, the suspension was filtered on a Büchner funnel connected to a vacuum pump and rinsed with deionized water until neutrality. Then two aqueous solutions of 25 kDa branched polyethylenimine (bPEI) (10 g in 20 ml, 1 : 2 ratio w% compared with cellulose) and anhydrous citric acid (CA) (2.556 g in 20 ml – amount calculated by means of **Equation 4**) were slowly added to the TOCNF solution, while continuously stirring until obtaining a white and homogeneous hydrogel. This latter was placed in well-plates, quickly frozen at -35 °C, frozen-dried for 48 hours using a lyophilizer (at -52 °C temperature and 140 µbar pressure) and then thermally treated in the laboratory oven at a maximum temperature of 102 °C for 16 h. At the end of the process, CNS were grinded with a mortar and then washed with water to remove the excess bPEI.

$$\text{Mass of citric acid} = 10 \text{ g} * 7.39 \frac{\text{mmol}}{\text{g}} * 0.18 * 192.12 \frac{\text{mg}}{\text{mmol}} = 2556 \text{ mg} \quad [4]$$

(where 7.39 mmol/g is the concentration of p-NH<sub>2</sub> in bPEI)

#### 2.1.4 Preparation of heterogeneous catalyst CNS-Pd

After washing and drying, CNS were grinded into a fine powder. In the meantime, a saturated solution of PdCl<sub>2</sub> in 0.1 M HCl was prepared. Grinded CNS were then CNS were immersed in this solution until complete adsorption of Pd (10 minutes), repeating the adsorption cycle three times. After every sorption cycle, Pd-loaded CNS were filtered on a Büchner funnel and let dry at open air, finally obtaining the catalyst CNS-Pd.

## 2.2 Characterization

### 2.2.1 SEM and EDS Analysis

high vacuum scanning electron microscopy (SEM) analyses were performed to characterize the internal morphology of CNS and to obtain the high magnification images.

Energy dispersive X-ray spectroscopy (EDS) is an analytical tool for elemental analysis and chemical characterization. This method analyzes by collecting X-rays from an X-ray machine or other X-ray source that interact with the sample. Since different elements have different emission spectra due to different atomic structures, the different components contained in the sample can be distinguished by analyzing the X-ray spectrum, which can be used to determine the elemental composition in the sample. In this study, EDS was used to determine the content of different atoms distribution in CNS-Pd. This operation takes place at 20keV

### 2.2.2 ICP-OES and Leaching test

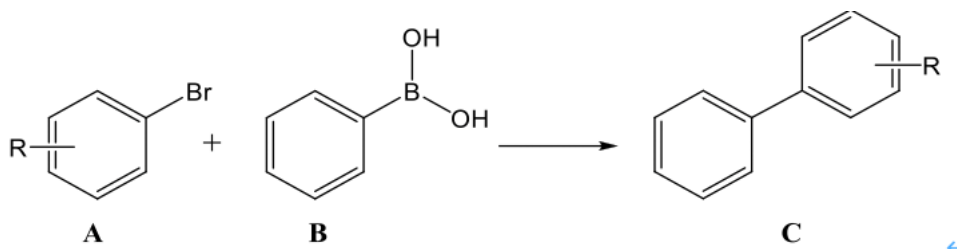
Metals concentration was measured by inductively coupled plasma optical emission spectroscopy (ICP-OES), using a Perkin Elmer Optima 3000 SD spectrometer in LAC (Laboratorio Analisi Chimiche, Politecnico di Milano).

Leaching test has been done for blank sample and the sample after reaction in aqueous samples. Put 1 mg of CNS and CNS-Pd into 2.5 ml of water in a vial respectively, add the reactants and other reagents involved in the reaction, and react in a microwave reactor at 100 °C for 30 min. The filtrate was subjected to ICP-OES test to quantitatively confirm the concentration of Pd contained. All the data can be used for calculate the percentage of loosing quantity of catalysts loading. thanks to inductively coupled

plasma optical emission spectroscopy (ICP-OES), using a Perkin Elmer Optima 3000 SD spectrometer in LAC (Laboratorio Analisi Chimiche, Politecnico di Milano).

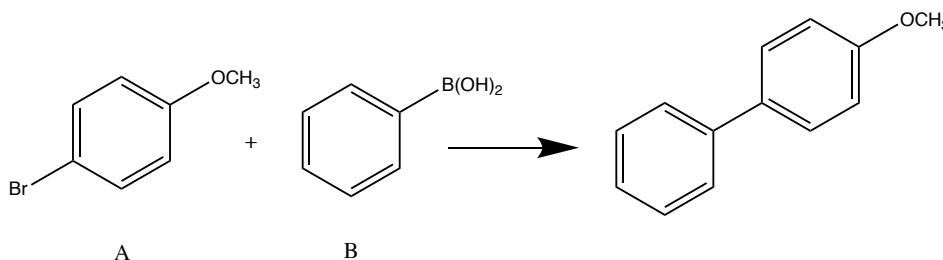
## 2.3 Suzuki-Miyaura coupling

### 2.3.1 Basic standard reaction



Scheme 1. Suzuki-Miyaura reaction.  
R= OCH<sub>3</sub>, CH<sub>3</sub>, Br, H, CN.

The scheme 1 shows the expression of the Suzuki reaction. For the convenience of research, we choose the following reaction as the standard reaction to be studied according to the references.



Scheme 2. Basic standard reaction for Suzuki-Miyaura reaction studying.

In a 2-5 mL microwave vial, CNS-Pd (2-10% w/w compared to reagent **A**), KOH (2 eq), reagent **B** (1.5 eq) and 2.5 mL of water as solvent were added. Then, TBAB (0.15 – 0.6 eq) and reagent **A** (1 eq) were put in the vial. The reaction was performed under microwave irradiation in a temperature range of 40-130°C and for reaction times between 10 minutes and 1 hour.

### 2.3.2 Reaction treatment and product purification

At the end of the reaction, 2 ml of ethyl acetate were added in the reaction mixture and stirred for 10 minutes. The solution was then filtered in a glass straw equipped with cotton to remove the catalyst and the reaction vial was washed three times with 2 ml

of water and three times with 2 ml of ethyl acetate. The organic and aqueous phases were transferred in an extractor funnel and 5 ml of 0.1 N HCl solution were added. The aqueous phase was then extracted three times with 15 ml of ethyl acetate and all the organic phases were collected together and then dried with Na<sub>2</sub>SO<sub>4</sub>. The final organic solution was then filtered off and the solvent was removed under vacuum to obtain a crude which was analysed by <sup>1</sup>H-NMR and GC-MS analysis (see Section 2.5). The purification of the product was performed with flash column chromatography, using a solvent mixture of hexane and ethyl acetate in a 95 : 5 ratio.

Yields can be obtained by calculating the area from <sup>1</sup>H-NMR with internal standard. That can be detailed by following methods. After exploring the reaction conditions, silica gel column chromatography was performed directly to obtain yields by weight of product compared to crude product

**Internal standard:** it is a convenient way to measure the real yield. In this study case, acetonitrile can be used as the internal standard, and generally use the ideal quantity of equivalent or 1/2 equivalent. In this study. Firstly, it is be needed to prepare the internal standard solution: dissolve 14.1ul acetonitrile in deuterated chloroform to make it as 1 ml solution by using volume flask, then every 0.1ml of this solution has 0.267mmol of acetonitrile inside, which is the same quantity of ideally converted product. Secondly, make the crude as a certain volume solution for example 100 ml, so withdraw 10 ml to remove the solvent and added to the <sup>1</sup>H-NMR tube with 1/10 (0.1ml) of the internal standard solution, and the yield was calculated by the area ratio of the spectrum. The amount of target products in the NMR sample tube can be known by internal standard, and the actual yield can be obtained after the amplification and converted.

### 2.3.3 Condition optimization

#### Temperature and Time.

According to the experimental requirements, adjust the reaction time of the microwave reactor, while keeping other conditions unchanged, change the time and temperature respectively, the time range is 0.5-1h, and the temperature range is 25°C-130°C.

#### Base, catalyst and TBAB

Under the known and determined external conditions (temperature, reaction time), control experiments were carried out for the base, the amount of catalyst, and TBAB, respectively. The amount of catalyst used in the experiment was 2%, 5%, 10%, 100%, 50%, 25% of the base reaction amount used for TBAB.

### 2.3.4 Recycling and Reuse

In a 2-5 mL microwave vial, CNS-Pd (2% w/w compared to reagent A), KOH (2 eq), reagent B (1.5 eq) and 2.5 mL of water as solvent were added. Then, TBAB (0.15 eq) and reagent A (1 eq) were put in the vial. The reaction was performed under microwave irradiation at 100 °C for 30 minutes. Then, CNS-Pd was recovered by filtration and reused for the same reaction for five cycles in the same reaction conditions. After a proper work-up (see Section 2.3.1.) every reaction was analysed by <sup>1</sup>H-NMR with an internal standard to verify the reusability efficiency of the catalyst.

### 2.3.5 Scope of reaction

To explore the versatility of the CNS-Pd catalyst prepared in this study, it is applied halogenated aromatic hydrocarbons with different substituent groups in the synthesis, including 4-bromobenzaldehyde, 4-bromotoluene, 4-bromo benzene, 1,4-dibromobenzene, 4-bromoaniline, 2-bromobenzonitrile, 1,3,5-Triphenylbenzene. For the amount of reagent, it is proportional to the basic reaction (50 mg)







## 3. Result and Discussion

### 3.1 Materials and Products

The TOCNF obtained after oxidation presents a flocculent shape. In fact, after the cellulose is oxidized by the sodium hypochlorite system, the original hydroxyl groups become carboxyl groups. Due to electrostatic force and intermolecular force, when dispersed in the water phase, the whole system presents a homogeneous dispersed phase with long fibers.. Finally, we obtained the oxidation degree of TOCNF is 1.304

$$\frac{mmol_{COOH}}{g_{TOCNF}}$$

In order to obtain the desired micro-/nano-porous architecture, water was added to



Figure 11. TEMPO-oxidized cellulose nanofibers from cotton linters

the mixture, which was then frozen and lyophilized, leaving cavities in the CNS structure. Further heat treatment is to make the crosslinks tighter and increase the strength of the aerogel. Washing is to remove CA and bPEI that are not involved in cross-linking. According to the work from O<sup>SCM</sup>Lab [61], with the different application ratios of bPEI and TOCNF in CNS, we can obtain CNS with different mechanical

strengths. As shown in the figure 12, the ratios of cellulose/bPEI are 1:1 and 1:2 respectively. We can clearly see that more cross-linking agent (bPEI) makes the CNS have stronger mechanical strength and the more complete overall morphology

In order to obtain the desired micro-/nano-porous architecture, water was added to the mixture, which was then frozen and lyophilized, leaving cavities in the CNS structure. Further heat treatment is to make the crosslinks tighter and increase the

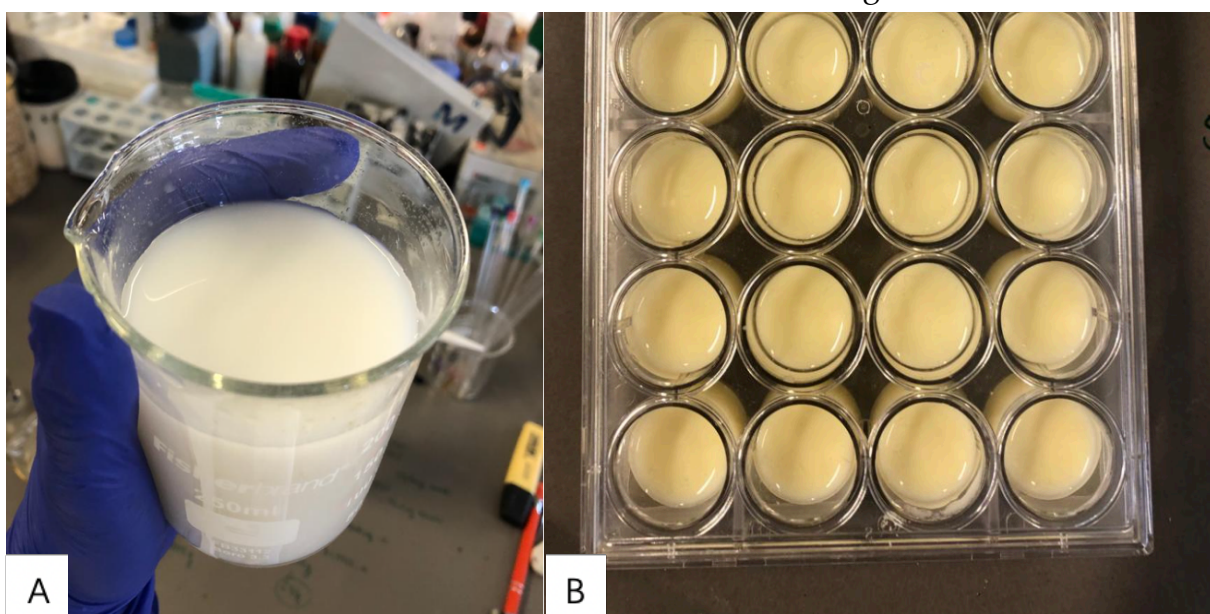


Figure 12. Water suspension of sonicated TOCNF (A), mixture of TOCNF, bPEI and citric acid (B)

strength of the aerogel. Washing is to remove CA and bPEI that are not involved in cross-linking. According to the work from O<sup>SCM</sup>Lab [61], with the different application ratios of bPEI and TOCNF in CNS, we can obtain CNS with different mechanical strengths. As shown in the figure 12, the ratios of cellulose/bPEI are 1:1 and 1:2



*Figure 13. Comparison of CNS morphology prepared with different TOCNF: bPEI ratio, for 1:2 (left) and 1:1 (right)*

respectively. We can clearly see that more cross-linking agent (bPEI) makes the CNS have stronger mechanical strength and the more complete overall morphology

The catalysts we used in the follow-up research are mainly CNS carrying palladium ions. In fact, the chelating action of amino group from bPEI lock the palladium ions from palladium chloride, and its effect is similar to the role of long chain or macromolecules in common palladium catalysis complexes. The reason why using CNS with a cellulose/bPEI ratio of 1:1 in this study is that the Pd loading only require powdered carriers for reaction, and lower content of bPEI are environmentally friendly options<sup>[60]</sup>. After grinding and pulverizing, we can see that the more finely divided CNS powder is pale yellow. After dissolving the palladium chloride powder in the HCl solution, we poured the crushed CNS into the solution for stirring and

filtered, after drying and washing, the color of the dried catalyst changed from pale yellow to yellow-brown due to palladium loading. During the preparation of the catalyst, we can also see that the color of the HCl solution changes from yellow at the beginning to a clear pale yellow.

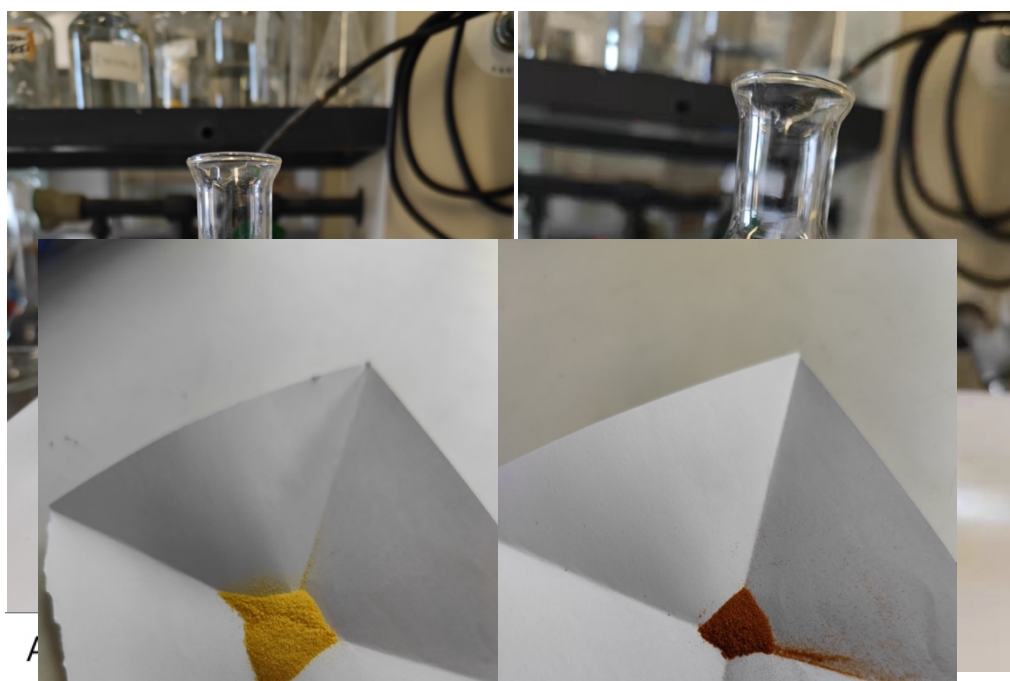


Figure 15. Color change of palladium chloride solution before (A) and after (B) absorption



Figure 14. CNS (A) and CNS-Pd (B)

## 3.2 Materials characterization

### 3.2.1 SEM and EDS analysis

It can be seen from SEM that the obtained CNS has more layered structure and obvious porous structure in some areas, which provides a larger specific surface area for the subsequent implementation of catalyst particles, and also improves the catalytic performance.

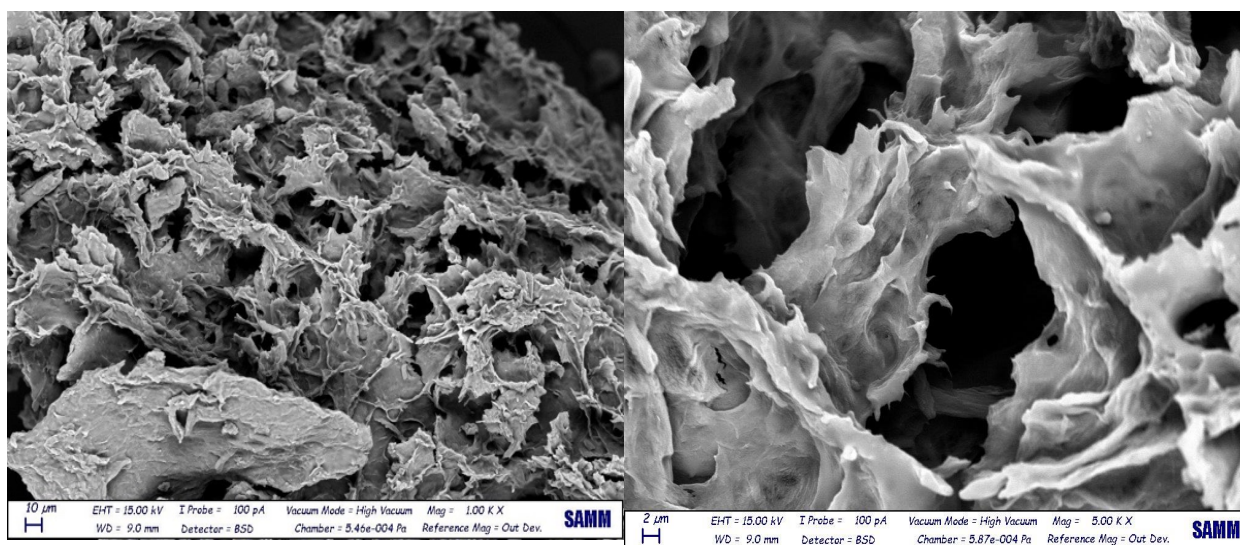


Figure 16. SEM images of CNS-Pd: 10 $\mu$ m and 2 $\mu$ m

From the EDS detection results, it can be seen that after the palladium chloride particles are fully absorbed, a high concentration of effective catalytic components is uniformly distributed throughout the CNS. Except for the actively carried palladium chloride, according to the spectrum, the content of other metal impurities is little or no, which confirms the high absorption capacity of CNS (Figure 16).

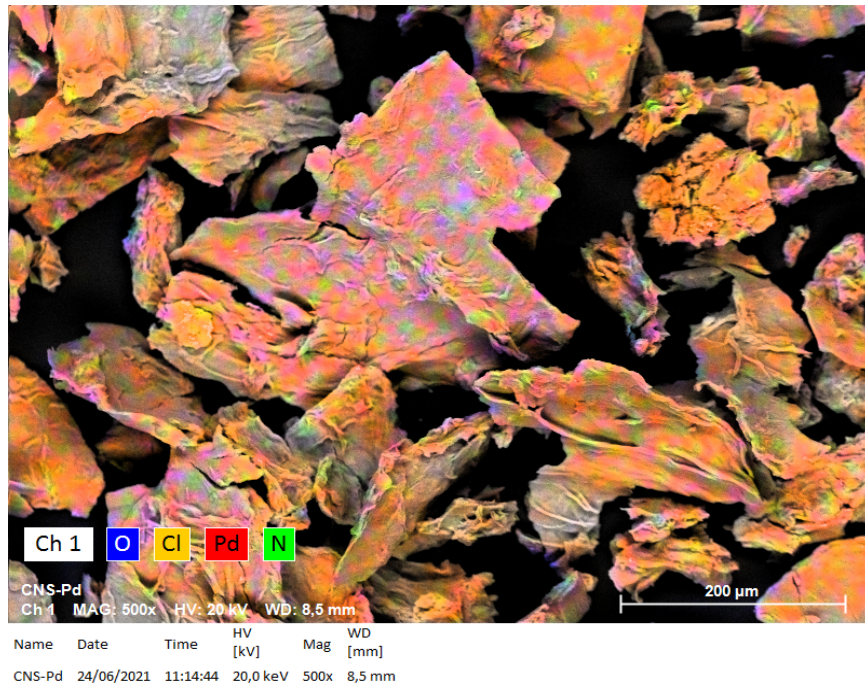


Figure 17. EDS image of CNS-Pd

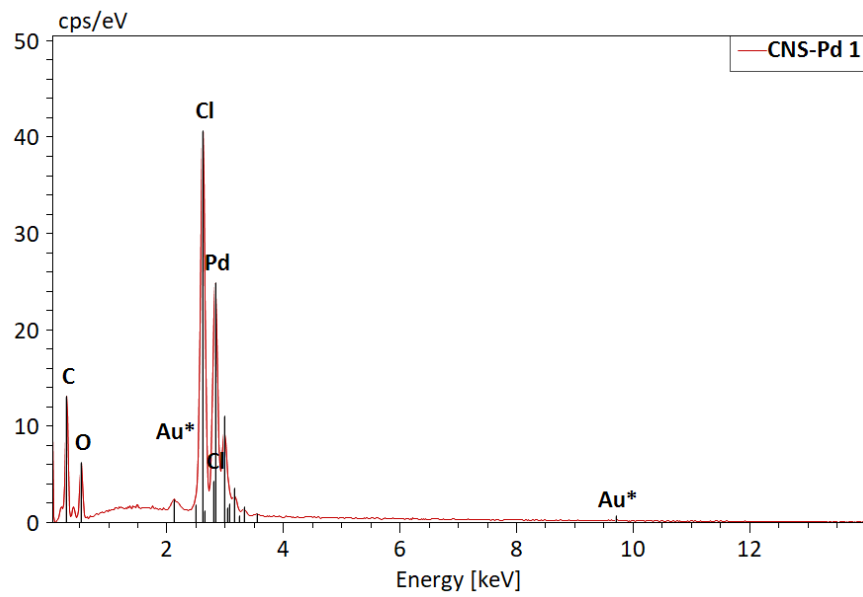


Figure 18. EDS absorption spectrum of CNS-Pd



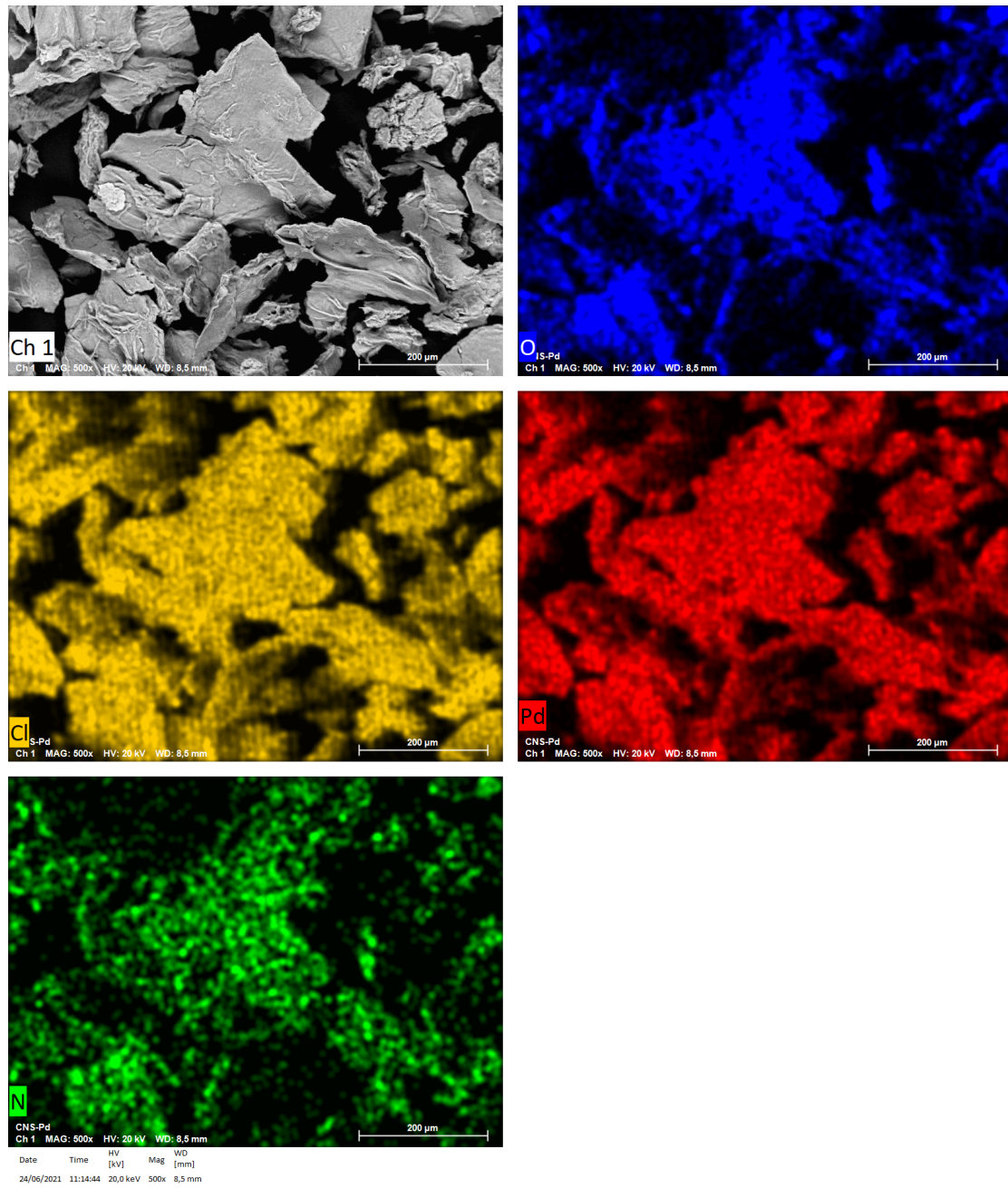


Figure 19. Distribution map of different elements of CNS-Pd

### 3.2.2 ICP-OES and Leaching test

CNS-Pd was characterized by ICP-OES measurements to further confirm the presence of palladium in the synthesized material and quantify the loading. As shown in Table 1, the analysis reported significant palladium concentrations. This result confirms that the CNS adsorption and loading of palladium chloride particles is successful, and it has certain catalyst characteristics.

Table 1. Pd loading concentration on CNS-Pd

Sample	Pd (w%)
CNS-Pd	22.7 ± 0.4

After performing leaching tests of blank CNS and reacted CNS-Pd, we can find that the CNS prepared in this study does not have any palladium metal loading itself. After one reaction, there is some hypotheses such as thermal motion or redox changes, the palladium metal carried by the CNS will be leached to a trace extent.

Table 2. Pd concentration on Leaching test

Sample	Pd (mg/L)
Leaching-Blank	<0.01
Leaching-Pd	12.67 ± 0.5

The leaching amount is less compared to the loading amount, which can be calculate in Equation 5:

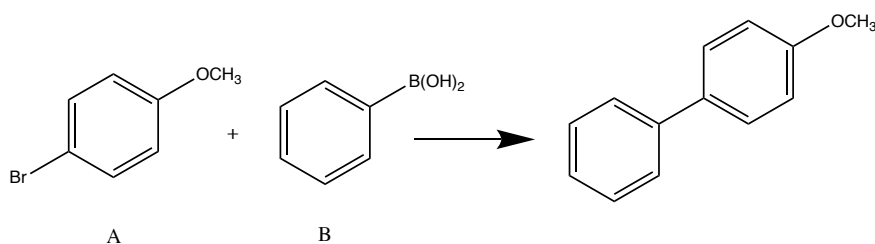
$$\text{Leaching degree} = \frac{2.5\text{ml} \times 12.67 \text{ mg/L}}{1 \text{ mg} \times 22.7 \text{ w\%}} = 0.1395\% \quad [5]$$

With the calculation results, we can see that in the actual reaction process, due to the good chelating ability of CNS, more than 98% of the Pd loading of CNS-Pd can be

“locked”, and in the subsequent reuse process, the reuse also shows that the catalytic activity of the catalyst did not lose too much due to leaching.

### 3.3 Yield and conversion

Depending on the basic reaction we choose, we first analyze the product yield and conversion of the reaction. According to the process of Suzuki reaction, we can easily get the following basic reaction:



*Scheme 2. Basic sample of Suzuki-Miyaura reaction*

According to the internal standard method described in 2.2, we take 1/10 of the amount for product to analysis. Since we can select any methyl group in the product, compare the methyl group peaks of acetonitrile, presented by adding a certain amount of acetonitrile to obtain the area ratio of the methyl peaks between the internal standard and the product  $q$ , thus inferring the yield  $y$  can be calculated by **Equation 6**:

$$y = \frac{2 \cdot 10 \cdot n(\text{Acetonitrile})}{n(\text{Bromoanisole}) \cdot q} * 100\% \quad [6]$$

After the reaction, the pure product was obtained by using a silica gel chromatographic column, and after calculation, it was known that the yield calculated according to the product mass was 97%. This basically agrees with internal standard calculations, so we can assume that internal standard method is suitable for measuring this response. In summary, our calculation has a high degree of confidence and can be used as a judgment based of the degree of reaction.

## 3.4 Optimization condition

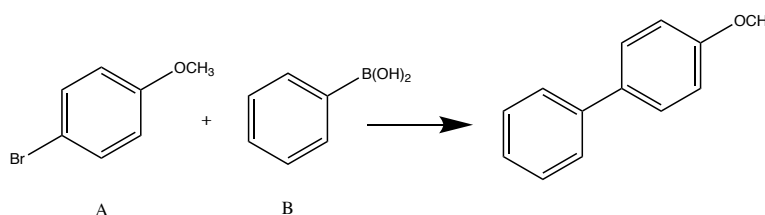
### 3.4.1 Time and Temperature

Compared with conventional heating, microwave heating is one of the most useful tools in organic synthesis because of its obviously advantages of fast heating, thermal efficiency, saving energy, clean, and easy operation. Palladium catalyzed Suzuki-Miyaura cross-coupling reaction could tolerate a broad range of functional groups with high stereoselectivity to provide a mild method in preparation of kinds of substituted biaryls.

Usually, the Suzuki-Miyaura cross-coupling reaction is mostly carried out by conventional heating methods, and it usually takes several hours to dozens of hours to complete the reaction. In 1986, Gedye<sup>[38]</sup> and Giguere et al.<sup>[63]</sup> first used microwave heating. The application of this method to organic synthesis greatly shortens the reaction time of conventional organic synthesis, which is favored by synthetic chemists. After that, a large number of literatures and review articles on microwave synthesis chemistry appeared<sup>[64][65][66]</sup>. Subsequently, the application of Microwave technology to promote the study of Suzuki-Miyaura cross-coupling reaction has set off an upsurge in the chemical community.

In this project study, we optimized the reaction time and temperature to the following ranges according to the work of Kamal M. Dawood<sup>[67]</sup>, in which, as a control group, the reaction at room temperature and conventional heating mode

were also added. And the basic reaction is:



*Scheme 2. Basic sample of Suzuky-Miyaura reaction*

Thanks to the use of microwave reactors, we can optimize the reaction time and temperature to save resource consumption and optimize reaction conditions. We selected the temperature of 25°C, 40°C, 80°C, 100°C, 130°C, and the time of 48 h, 24 h, 30 min, and 20 min respectively as the gradient of the experimental conditions, adhering to the principle of "time-temperature equivalence", shortening the reaction time under the condition of increasing temperature, considering energy consumption, safety and other reasons, The purpose of the test is to obtain the best reaction conditions

Table 3. Reaction result for different time and temperature

Entry	T	t	Nmr
1	100 °C	30 min	92%
2	80 °C	30 min	57.%
3	100 °C	20 min	71.5%
4	25°C	48 h	39.3
5	80	30	46%
6	100	20	53%

\*50 mg 4-bromoanisole and 48.89 mg phenylboronic acid reacted in 2.5 ml water under MW reactor

\*\*Entry 5 and Entry 6 have same condition without TBAB

We can compare that under the conditions of 25°C and 40°C, the degree of reaction is very low, and the raw materials 4-bromanisole and phenylboronic acid are clearly visible in the spectrum. Under the conditions of 80°C and 100°C, it is obvious that the degree of reaction of 100°C is higher. , adding the internal standard material to calculate the yields respectively, it can be seen that under the same reaction time, the reaction degree of 100°C is higher. For the requirements of energy saving and greenness<sup>[60]</sup>, although the reaction degree is also high at 130°C, the reaction degree of 100 °C is higher enough and Yields have already met expectations.

According to the yield calculation results, we can see that at the same temperature, the longer the reaction time, the greater the product yield, and after 30 min, the basic yield can reach more than 95%, so we select the reaction condition on the basis of data as 30 min 100°C . As a control group, we also tested the reaction at room temperature (25) for 48 hours, and the reaction results showed that the whole reaction system always needs a higher temperature as initiation.

### 3.4.2 Catalyst, Base and TBAB

Kabalka's research group<sup>[70][71]</sup> deposited 5 mol% palladium powder on Al<sub>2</sub>O<sub>3</sub>, and used this as a catalyst, KF as a base, and under the action of microwave, the Suzuki-Miyaura cross-coupling of aryl halide and arylboronic acid was carried out. In 2004, Sauer et al.<sup>[72]</sup> used functionalized fiber-supported palladium (Fibre-Cat) and polystyrene-supported palladium (PS-PPh<sub>3</sub>-Pd) as catalysts in the presence of K<sub>2</sub>CO<sub>3</sub>, EtOH as solvent, and microwave irradiation. The Suzuki-Miyaura cross-coupling reaction of various halogenated aromatic hydrocarbons and different arylboronic acids was successfully catalyzed within 10-25 min.

Compared with the existing results, the biggest highlight of our work is that the participation of organic solvents is eliminated, the reaction is carried out in pure water phase reaction, and heterogeneous catalysis is realized at the same time. After determining the appropriate external conditions for the reaction, we compared the effect of catalyst dosage, base type and phase transfer agent dosage on the reaction. The hypothesis considered are:

- i. In order to achieve the goal of green chemistry, the introduction of too many other compounds into the system should be minimized
- ii. In order to obtain high-purity products in the future, improve the yield and reduce the difficulty of treatment of the reaction

- iii. Optimize the reaction system and try to broaden the application conditions of the Suzuki reaction

The first thing to optimize is the amount of catalyst used. It is obvious that the more catalyst in the system, the greater the catalytic efficiency and the faster the reaction proceeds. We control the amount of catalyst at 2%, 5%, and 10% to calculate the yield of the reaction, and we can get the following reaction results:

Table 4. Reaction result for different catalyst percentage

Entry	Cat.(w%)	Base(%)	TBAB(%)	Nmr
1	2%	1	1	92%
2	5%	1	1	95%
3	10%	1	1	94%
4	0	1	1	0%

\*50 mg 4-bromoanisole and 48.89 mg phenylboronic acid reacted in 2.5 ml water under MW reactor with full TBAB and Base

It can be clearly seen from the experiment that the reaction does follow the principle of "the more catalyst is used, the more complete the reaction is", but in terms of yield, the gap between the three is not large. The yield difference was within  $\pm 3\%$  calculated by the method of internal standard. We observed that when the catalyst dosage was increased from 5% to 10%, the yield decreased slightly. The initial guess inferred that the reason is: since the amount of base in the system is fixed, more catalyst dosage means that it can be converted into The amount of palladium(0) particles is fixed, and more palladium(II) is not reduced, so it cannot participate in the Suzuki reaction. These unreduced palladium(II) particles hinder the contact between the catalyst and the reactants, which affecting the catalytic efficiency.

As the main reactant, the function of base is to provide the basic environment required for the coupling reaction. When we explored the amount and type of base, we found



that the amount of base must be slightly more than 1 equivalent, and for different bases, we see that it is very weak. Therefore, NaOAc, Na<sub>2</sub>CO<sub>3</sub>, K<sub>2</sub>CO<sub>3</sub>, KOH are considered. The nanocellulose aerogel used in this study contains a large number of theoretical basic groups in the carrier due to the reaction with the cross-linking agent(bPEI), so we also tested whether the base-free system can be used, and tried to use The support material (cross-linked oxidized cellulose aerogel) acts as a supporter for the alkaline environment. The experimental results are as follows:

Table 5. Reaction result under the influence of base existence

Entry	T	t	Cat.	Base(%)	TBAB(%)	Nmr
1	100 °C	30 min	2%	1	1	92%
2	100 °C	30 min	2%	0	1	54%
3	100 °C	30 min	10%	0	1	55%
4	RT	48 h	2%	0	1	25%
5	100 °C	30 min	2%	0	0	0

\*50 mg 4-bromoanisole and 48.89 mg phenylboronic acid reacted in 2.5 ml water under MW reactor

Experiments show that NaOAc, Na<sub>2</sub>CO<sub>3</sub>, K<sub>2</sub>CO<sub>3</sub> and other salts cannot provide a sufficient alkaline environment in the reaction system, and the catalyst reduction is poor. If no alkali is added, only the oxidized cellulose aerogel itself cannot provide a enough alkaline environment. , the product conversion rate is low. And only more reagent peaks show in spectrum.

The use of microwave to promote the Suzuki reaction in aqueous phase has been successfully applied in industrial production. In 2002, Barbarell first used Pd(OAc)<sub>2</sub> as the catalyst, TBAB as the auxiliary agent, and the Suzuki reaction was used to finally obtain the hexameric thiophene product. According to the reaction contained in the literature<sup>[67]</sup>, TBAB is used as a phase transfer agent, mainly to help the reactants enter the water phase, so that the reaction can be carried out in the water phase. But the

problem is that in the process of subsequent reaction treatment, due to the existence of hydrophilic groups and hydrophobic groups of TBAB, it is not easy to remove during the extraction process, which easily affects the purity of the product,. So the optimized operation is the amount of TBAB from 1 to 25% equivalent. This try is to reduce the amount of TBAB, and the results are as follows showing:

Table 6. Reaction result for different TBAB percentage

Entry	Base(%)	TBAB(%)	Nmr
1	1	1	92%
2	1	0.5	96.5%
3	1	0.25	97%
4	1	0	90%
5	0	0	0

\*50 mg 4-bromoanisole and 48.89 mg phenylboronic acid reacted in 2.5 ml water under MW reactor

The results showed that the reaction yield was higher when using 25% TBAB in the basic reaction, but the yield difference was about  $\pm 5\%$  from 100% to 25%.

### 3.4.3 Amplify the reaction

The purpose of realizing industrial application is to experiment from small amounts of trace reactions to medium or large amounts of reactions. After obtaining the optimal reaction conditions through a series of experiments, the next step is to expand the scope of the reaction proportionally to explore whether the reaction can complete a large-scale experiment under the determined conditions 100°C and 30 min.

In the scaled-up reaction, the experimental conditions were kept as previous, after scaling up the amount of solvent and reactants used tenfold, we obtained 95% yield (w/w) after purification by column chromatography. However, after processing the reaction, it can be significantly found that the yield shown by GC-MS is only 39.83%.

It is speculated that some reactants are still left due to insufficient reaction time. At the same time, after amplifying the reaction, more impurities are introduced, which may affect the reaction.

#### 3.4.4 Recycling and reuse

In 2004, Hu's group<sup>[68]</sup> prepared a stable poly(N,N'-dihexyl)imide-supported nanopalladium complex (PDHC-Pd) with an average size of about 3 nm. They used this complex as a catalyst. Dioxane was used as solvent, K<sub>2</sub>CO<sub>3</sub> was used as base, and the reaction was carried out under microwave irradiation for 40 min. The Suzuki-Miyaura cross-coupling reaction between iodobenzene and phenylboronic acid could be carried out smoothly, and the yield of the coupling product could reach 95%; For the same target yield, conventional heating takes 20 h. Although the catalyst can be recycled for more than 5 times, the catalytic activity decreases slightly after each recovery.

Table 7. Catalysts recovery rate for reuse

T	t	Remark	Result
100 °C	30 min	first	Recovery 72%
100 °C	30 min	second	Recovery 80%
100 °C	30 min	third	Recovery 45%

The CNS-Pd catalyst prepared in this study, as a porous stable structure, directly avoids the structural change caused by the excessive number of cycles of conventional palladium-catalyzed ligands. In order to explore the actual use and the number of cycles, we amplified the reaction five times, and also recovered the catalyst powder after the reaction, rinsed with ethyl acetate and water, and dried it for the next cycle.

Table 8. Yield result for reuse

T	t	Remark	Yield
100 °C	30 min	I	99%
100 °C	30 min	II	83%
100 °C	30 min	III	65%
100 °C	30 min	IV	63%

After experiments, we know that the CNS-Pd catalyst prepared in this study has good recovery and reuse characteristics. After four cycles, more than 60% conversion was still achieved, demonstrating the long catalyst life. At the same time, it can still maintain an average recovery rate of more than 65.67% after recycling, which reflects sufficient environmental protection and economic value.

### 3.4.5 Scope of reaction

The biggest advantages of Suzuki reaction are mild reaction conditions, high conversion efficiency, and substrate universality. organoboron reagents are stable, low toxicity and widely available<sup>[69]</sup>. After experiments, we can see that the catalysts prepared in this study are suitable for the Suzuki reaction. They have different catalytic activities for different substituents, but they all show a catalytic activity. They have a similar electronic arrangement to that of 4-bromoanisole. , the catalytic activity is slightly better than others, which shows some limitations, but also provides ideas for follow-up research.

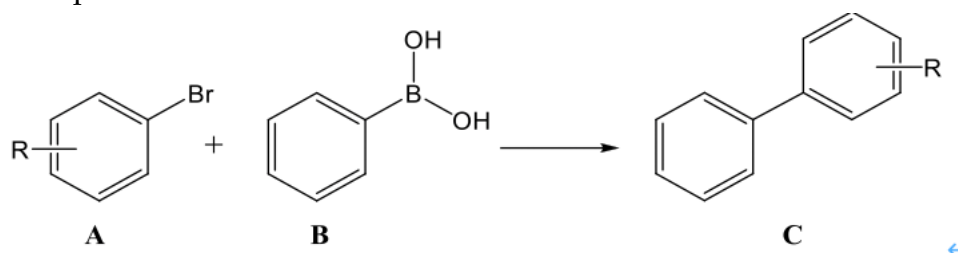


Table 9. Reactions with different substituents

Entry	A	C	Conversion*
1	4-bromobenzaldehyde	4-Formylbiphenyl( <b>e</b> )	<3%
2	4-bromotoluene	4-Methylbiphenyl( <b>f</b> )	67.3%
3	4-bromo benzene	Biphenyl( <b>g</b> )	28.4%
4	1,4-dibromobenzene	p-Terphenyl( <b>h</b> )	27.6%
5	4-bromoaniline	4-Aminobiphenyl( <b>i</b> )	<7%
6	2-bromobenzonitrile	2-Phenylbenzonitrile( <b>j</b> )	58%
7*	1,3,5-Triphenylbenzene	1,3,5-Triphenylbenzene( <b>k</b> )	43%

\* Entry 7 is reacted for 1h

\*\* Conversion is calculated by GC-MS since there is solubility problem for Nmr preparation

## 4. Conclusion and Outlook

Using cellulose as the protagonist, starting from the modification of cellulose, cellulose is oxidized and made into Tempo-oxidized cellulose nanofibers(TOCNF). Under the co-crosslinking effect of CA and bPEI, vacuum freeze-drying and heat treatment are used to obtain cellulose nanosponges (CNS aerogels) with certain mechanical strength. After loading palladium chloride particles by adsorption, a composite material CNS-Pd with catalytic properties was obtained. The atomic distribution characteristics and microstructure of the material were obtained by SEM and EDS analysis, and it was confirmed that it has a layered and reticulated pore architecture and a relatively high comparative area. At the same time, the amount of Pd carried in the CNS-Pd was quantitatively confirmed by ICP-OES and leaching test.

The prepared and characterized CNS-Pd took the Suzuki reaction as the research object, explored the suitability and versatility of this new catalyst for the Suzuki reaction. Experiments have confirmed that this material has a good catalytic effect on the current Suzuki reaction. With the help of the microwave reactor, the Suzuki reaction with high conversion rate in the aqueous phase is completed. Meanwhile, according to the experiment, the optimal conditions were determined to be 100 degrees Celsius and 30 min. The variety and amount of alkali required by the system were also tested many times, and the conclusion was obtained that KOH was the optimal alkali salt. The dosage of TBAB and catalyst has also been verified in the experiment. Under the requirement of green chemistry, the dosage of 2% (w/w) catalyst and 25% (0.15

equivalent) of TBAB can also reach up to 97% of the reaction conversion. The scale-up reaction provides experimental verification for subsequent industrial applications, and the repetition rate of the conversion rate of more than 65% is obtained by repeating it four times. This catalytic material has good environmental friendliness and long service life. Experiments to explore the versatility were also carried out between brominated aromatic hydrocarbons with different substituents, and it was also known that CNS-Pd had catalytic efficiency in similar reactions.

Although the research on the Suzuki reaction has been completed, the catalytic effect of CNS-Pd is still worthy of expansion. At present, the application in the Heck reaction has achieved preliminary results, showing high catalytic activity. At the same time, the amplification reaction of the Suzuki reaction part and the detailed exploration of the amount of alkali are also the only way to realize industrial application and green chemistry. As of the end of this study, the CNS-Pd used has always been the same Pd content. For CNS-Pd with different strengths of CNS and different Pd loadings, how to make a unified dosage and accurately determine the required Pd content is as follows Phase I research content, which has profound implications for exploring the advantages of the high surface area ratio of the CNS.

## 5. Bibliography

- [1]. Kümmerer, 1st International Green and Sustainable Chemistry Conference, 2019.10.17
- [2]. Cefic Chemdata International 2018
- [3]. <https://www.compoundchem.com/2015/09/24/green-chemistry/>
- [4]. [https://ec.europa.eu/environment/strategy/chemicals-strategy\\_en#ecl-inpage-245](https://ec.europa.eu/environment/strategy/chemicals-strategy_en#ecl-inpage-245)
- [5]. [https://ec.europa.eu/info/strategy/priorities-2019-2024/european-green-deal\\_en](https://ec.europa.eu/info/strategy/priorities-2019-2024/european-green-deal_en)
- [6]. Schneider, N.; Lowe, D. M.; Sayle, R. A.; Tarselli, M. A.; Landrum, G. A. J. *Med. Chem.* 2016, 59, 4385.
- [7]. Miyaura, N.; Suzuki, A. *J. Chem. Soc., Chem. Commun.* 1979, 866.
- [8]. Liu, Q.-Y.; Zhang, L.; Mo, F.-Y. *Acta Chim. Sinica* 2020, 78, 1297
- [9]. Beller, M.; Blaser, H.-U. *Organometallics as Catalysts in the Fine Chemical Industry*, Vol. 42. Springer, Heidelberg, 2012.
- [10]. Bostroöm, J.; Brown, D. G.; Young, R. J.; Keseru, G. M. *Nat. Rev. Drug Discovery* 2018, 17, 709.
- [11]. Torborg, C.; Beller, M. *Adv. Synth. Catal.* 2009, 351, 3027.
- [12]. Liu, M.; Su, S.-J.; Jung, M.-C.; Qi, Y.; Zhao, W.-M.; Kido, J. *Chem. Mater.* 2012, 24, 3817.(b) *Org. Lett.* 2002, 4, 513.
- [13]. Lipton, M. F.; Mauragis, M. A.; Maloney, M. T.; Velez, M. F.; VanderBor, D. W.; Newby, J. J.; Appell, R. B.; Daus, E. D. *Org. Process Res. Dev.* 2003, 7, 385.
- [14]. Beletskaya, I. P.; Alonso, F.; Tyurin, V. *Coord. Chem. Rev.* 2019, 385, 137.
- [15]. He, Z.; Song, F.; Sun, H.; Huang, Y. *J. Am. Chem. Soc.* 2018, 140, 2693.
- [16]. Ohashi, M.; Saijo, H.; Shibata, M.; Ogoshi, S. *Eur. J. Org. Chem.* 2013, 2013, 443.
- [17]. Chen, L.; Sanchez, D. R.; Zhang, B.; Carrow, B. P. *J. Am. Chem. Soc.* 2017, 139, 12418.



- [18]. Z. Lei, Yang Chen, Guo Xuefeng, Mo Fanyang. *Organic Chemistry*, 2021, 41(09): 3492-3510.
- [19]. Wu Li, Long Yu, Ma Jiantai, Lv Gongxuan. *Molecular Catalysis*, 2019, 33(03): 263-273.
- [20]. Calo V, Nacci A, Monopoli A, et al. *J Org Chem*, 2005, 70(15): 6040-6044.
- [21]. Choudary B M, Madhi S, Chowdari N S, et al. *J Am Chem Soc*, 2002, 124(47): 14127-14136.
- [22]. Speziali M G, da Silva G M, de Miranda D M V, et al. *Appl Catal A: Gen*, 2013, 462: 39-45.
- [23]. Wimmer L, Rycek L, Koley M, et al. Springer, Cham, 2014. 61-157.
- [24]. Felpin F X, Ayad T, Mitra S. *Eur J Org Chem*, 2006, 2006(12): 2679-2690.
- [25]. Liu C, Rao X, Zhang Y, et al. *Eur J Org Chem*, 2013, 2013(20): 4345-4350.
- [26]. Firouzabadi H, Iranpoor N, Gholinejad M, et al. *RSC Adv*, 2011, 1(6): 1013-1019.
- [27]. Ma H, Cao W, Bao Z, et al. *CatalSciTechnol*, 2012, 2(11): 2291-2296.
- [28]. HUANG Cheng, LI Lai-geng. *Chinese Science Bulletin*, 2016, 61(34): 3623.
- [29]. DUNLOP M J, ACHA R YA B, BISESSU R. *Journal of Environmental Chemical Engineering*, 2018, 6(4): 4408.
- [30]. Dufresne, A. *Nanocellulose: from nature to high performance tailored materials*; Walter de Gruyter GmbH & Co KG: 2017; .
- [31]. Thomas, B.; Raj, M. C.; Joy, J.; Moores, A.; Drisko, G. L.; Sanchez, C. *Chem. Rev.* 2018, 118, 11575-11625.
- [32]. Kalia, S.; Dufresne, A.; Cherian, B. M.; Kaith, B. S.; Avérous, L.; Njuguna, J.; Nassiopoulou, E. *International journal of polymer science* 2011, 2011.
- [33]. Klemm, D.; Heublein, B.; Fink, H.; Bohn, A. *Angewandte chemie international edition* 2005, 44, 3358-3393.
- [34]. Zhao Bo, Hu Shang-lian, GONG Dao-yong, et al. *Chemical Industry and Engineering Progress*, 2017, 36(2): 555.
- [35]. SAITO T, ISOGAI A.I. *Coloids and Surfaces a-Physicochemical and Engineering Aspects*, 2006, 289(1-3):219-225.
- [36]. Isogai, A.; Saito, T.; Fukuzumi, H. *TEMPO-oxidized cellulose nanofibers. nanoscale* 2011, 3, 71-85.

- [37]. IWAMOTO S, KAI W, ISOGAI T, et al. *Polymer Degradation and Stability*, 2010, 95(8):1394-1398
- [38]. Gedye, R.; Smith, F.; Westaway, K.; Ali, H.; Baldisera, L.; Laberge, L.; Rousell, J. *Tetrahedron Lett.* 1986, 27, 279.
- [39]. DE NOOY A E J, BESEMER A C, BEKKUM V H, et al. *Macromolecules*, 1996, 29(20): 6541-6547.
- [40]. SHIBATA I, ISOGAI A. *Cellulose*, 2003, 10(2): 151-158.
- [41]. IWAMOTO S, NAKAGAITO A N, YANO H. *Applied Physics A*, 2007, 89(2):461-466.
- [42]. SAITO T, ISOGAI A. *Coloids and Surfaces a-Physicochemical and Engineering Aspects*, 2006, 289(1-3):219-225.
- [43]. SAITO T, HIROTA M, TAMURA N, et al. *Bio-macromolecules*, 2009, 10(7):1992-1996.
- [44]. SAITO T, HIROTA M, TAMURA N, et al. *Journal of Wood Science*, 2010, 56(3):227- 232.
- [45]. Song J K, Tang A M, Liu T T, Wang J F . *Nanoscale*, 2013, 5( 6) : 2482 .
- [46]. Lavoine N, Bergstrom L . *J . Mater . Chem .* , 2017, 5 ( 31 ) : 6105 .
- [47]. Laitinen O, Suopajarvi T, Osterberg M, Liimatainen H . *ACS Appl . Mater . Interfaces*, 2017, 9( 29) : 25029 .
- [48]. Ye C H, Malak S T, Hu K S, Wu W B, Tsukruk V V . *ACS Nano*, 2015, 9( 11) : 10887 .
- [49]. Mertaniemi H, Escobedo-Lucea C, Sanz-Garcia A, Gandia C, Makitie A, Partanen J, Ikkala O, Yliperttula M . *Biomaterials*, 2016, 82: 208 .
- [50]. Herrera M A, Mathew A P, Oksman K . *Cellulose*, 2017, 24( 9) : 3969 .
- [51]. Azeredo H M C, Rosa M F, Mattoso L H C . *Ind . Crops Prod.* 2017, 97: 664 .
- [52]. Moreau C, Villares A, Capron I, Cathala B . *Ind . Crops Prod.* 2016, 93: 96 .
- [53]. Oksman K, Aitomki Y, Mathew A P, Siqueira G, Zhou Q,
- [54]. Melone, L.; Rossi, B.; Pastori, N.; Panzeri, W.; Mele, A.; Punta, C. *ChemPlusChem* 2015, 80, 1408-1415.
- [55]. Fiorati, A.; Pastori, N.; Punta, C.; Melone, L. Mele, A., Trotta, F., Eds 2019.
- [56]. Fiorati, A.; Turco, G.; Travan, A.; Caneva, E.; Pastori, N.; Cametti, M.; Punta, C.; Melone, L. *ChemPlusChem* 2017, 82, 848-858.

- [57]. Fiorati, A.; Grassi, G.; Graziano, A.; Liberatori, G.; Pastori, N.; Melone, L.; Bonciani, L.; Pontorno, L.; Punta, C.; Corsi, I. *J. Clean. Prod.* 2020, 246, 119009.
- [58]. Paladini, G.; Venuti, V.; Almásy, L.; Melone, L.; Crupi, V.; Majolino, D.; Pastori, N.; Fiorati, A.; Punta, C. *Cellulose* 2019, 26, 9005-9019.
- [59]. Paladini, G.; Venuti, V.; Crupi, V.; Majolino, D.; Fiorati, A.; C. Punta, *Cellulose* 2020, 27, 8605-8618. 73
- [60]. Bartolozzi, I.; Daddi, T.; Punta, C.; Fiorati, A.; Iraldo, F. *J. Ind. Ecol.* 2020, 24, 101-115.
- [61]. L. Riva, C. Punta, A. Sacchetti, *ChemCatChem* 2020, 12, 6214.
- [62]. Butylina S, Tanpichai S, Zhou X J, Hooshmand S.; *Compos. Part A: Appl. S.* 2016, 83: 18 .
- [63]. Giguere, R. J.; Bray, T. L.; Duncan, S. M.; Majetich, G. *Tetrahedron Lett.* 1986, 27(41), 4945.
- [64]. Kappe, C. O. *Angew. Chem., Int. Ed.* 2004, 43, 6250.
- [65]. Leadbeater, N. E. *Chem. Commun.* 2005, 23, 2881.
- [66]. Dallinger, D.; Kappe, C. O. *Chem. Rev.* 2007, 107, 2563.
- [67]. Kamal M. Dawood \*, Mohamed R. Shaaban. *Arabian Journal of Chemistry* (2017) 10, 473–479
- [68]. Liu, Y. B.; Khemtong, C.; Hu, J. *Chem. Commun.* 2004, 398.
- [69]. Liu, Q.-Y.; Zhang, L.; Mo, F.-Y. *Acta Chim. Sinica* 2020, 78, 1297.
- [70]. Kabalka, G. W.; Pagni, R. M.; Wang, L.; Namboodiri, V.; Hair, C. M. *Green Chem.* 2000, 3, 120.
- [71]. Kabalka, G. W.; Wang, L.; Pagni, R. M.; Maxwell, H. C.; Vasudevan, N. *Synthesis* 2003, 217.
- [72]. Wang, Y.; Sauer, D. R. *Org. Lett.* 2004, 6, 2793.



# A. Appendix A

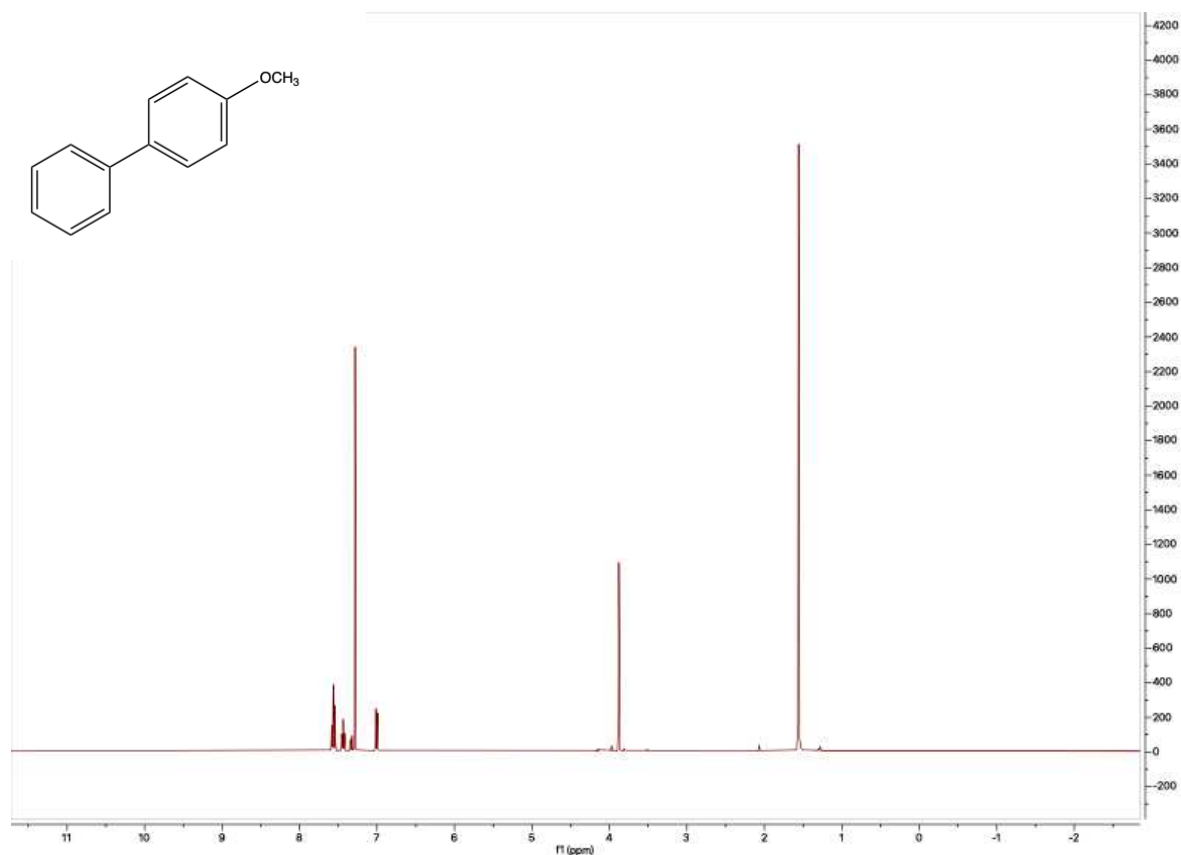
## Product spectrum

If we use 4-Bromoanisole and phenylboronic acid as reagent, For the final product “2.2.2. 4-Methoxy-1,10 -biphenyl”, its properties and the peak of products in the  $^1\text{H}$ -NMR spectrum are: Pale yellow powder; mp. 87–88 °C [Lit. mp. 87–88 °C (Zhang, 2004)];  $^1\text{H}$ -NMR ( $\text{CDCl}_3$ ) d 3.87 (s, 3H,  $-\text{OCH}_3$ ), 6.99 (d, 2H,  $J = 8.7$  Hz), 7.31–7.45 (m, 3H), 7.54 (d, 2H,  $J=9\text{Hz}$ ), 7.57 (d, 2H,  $J=7.2\text{Hz}$ ); MS m/z (%) 184 ( $\text{M}^+$ , 100), 169 (54.0), 141 (37.4), 115 (16.6), 89 (12.5), 76 (49.8), 63 (25.7)。

In this study, after purification, the product of basic reaction looks like



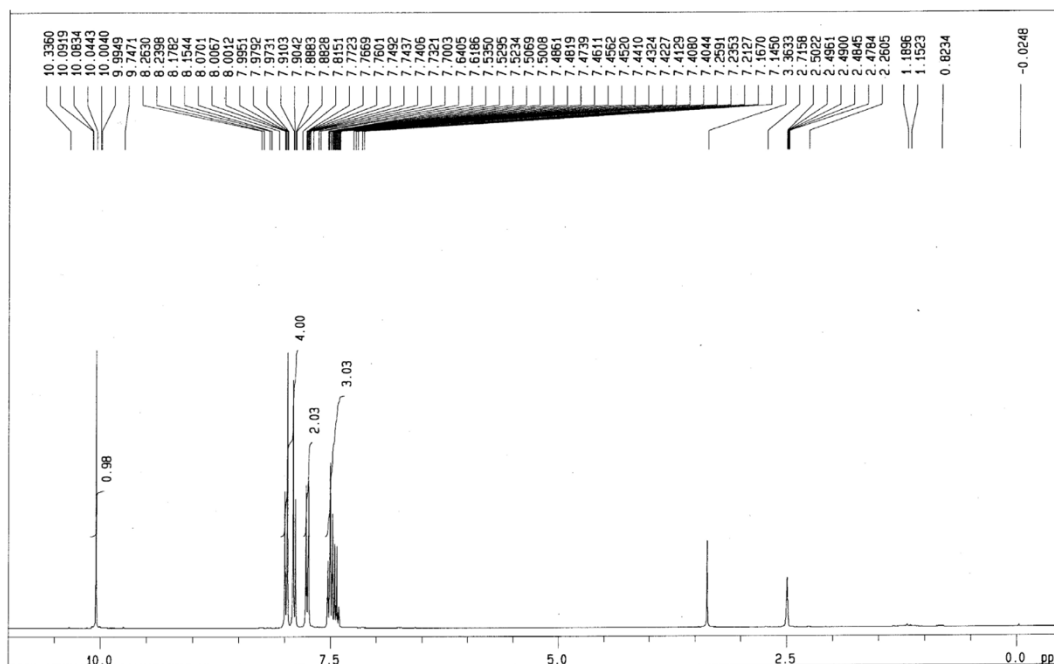
And the  $^1\text{H}$ -NMR spectrum can be clearly check after purification:



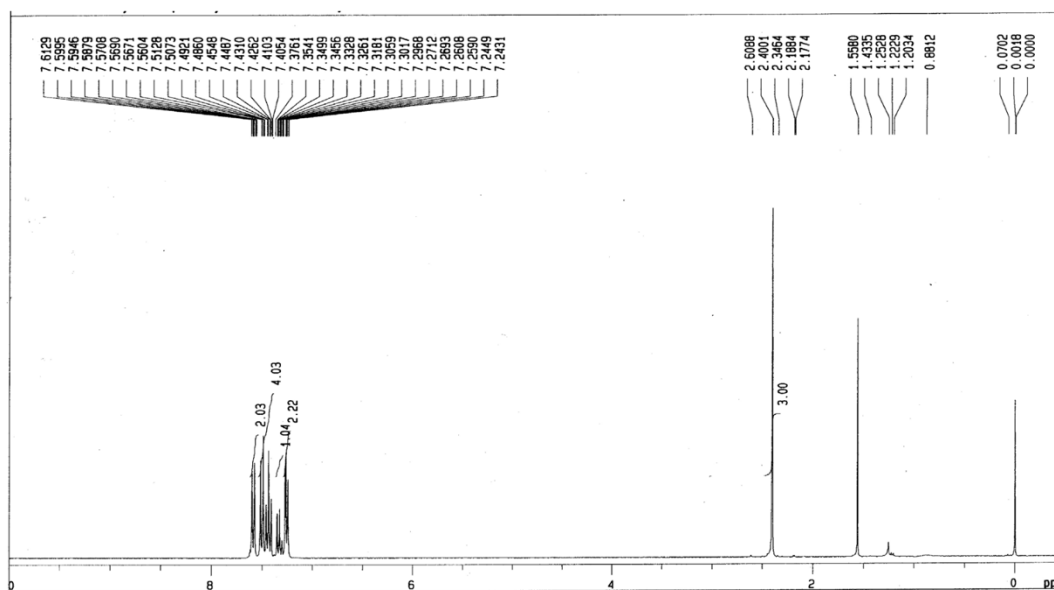
## Scope of reaction

For the reaction products mentioned in 2.2.4, the spectral information can be given by reference “Kim JH, Kim JW, Shokouhimehr M, Lee YS. Polymer-supported N-heterocyclic carbene-palladium complex for heterogeneous Suzuki cross-coupling reaction. *J Org Chem.* 2005 Aug 19;70(17):6714-20. doi: 10.1021/jo050721m. PMID: 16095291.”

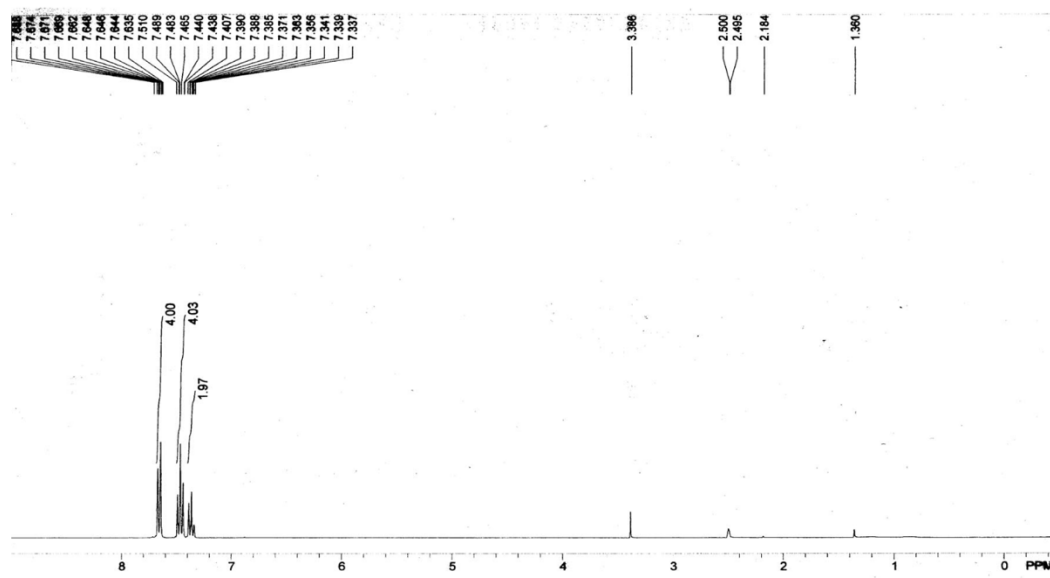
4-Formylbiphenyl(e).  $^1\text{H}$  NMR (DMSO):  $\delta$  (ppm) 7.48 (m, 3H), 7.74 (d, 2H), 7.91 (d, 2H), 8.00 (d, 2H), 10.04 (s, 1H). GC-MS:  $m/z$  182.



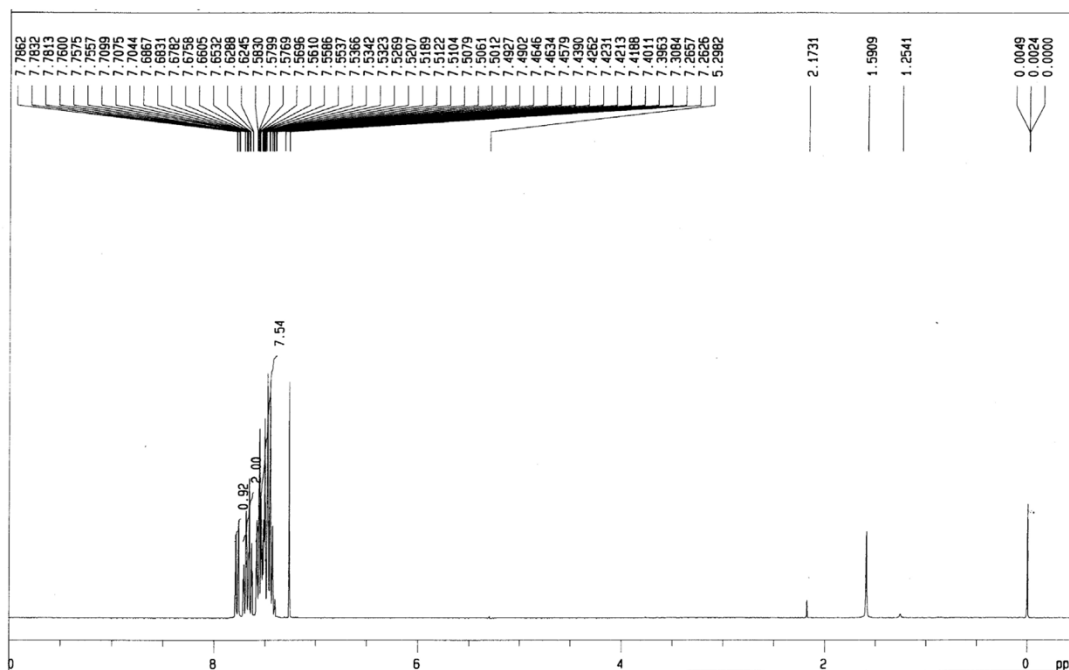
4-Methylbiphenyl(f).  $^1\text{H}$  NMR ( $\text{CDCl}_3$ ):  $\delta$  (ppm) 2.40 (s, 3H), 7.24 (d, 2H), 7.32 (q, 1H), 7.43 (q, 2H), 7.48 (d, 2H), 7.59 (d, 2H). GC-MS:  $m/z$  168.



Biphenyl(g).  $^1\text{H}$  NMR (DMSO- $d_6$ ):  $\delta$  (ppm) 7.33 (q, 2H), 7.44 (q, 4H), 7.64 (d, 4H). GC-MS:  $m/z$  154.



2-Phenylbenzotrile(j).  $^1\text{H}$  NMR ( $\text{CDCl}_3$ ):  $\delta$  (ppm) 7.50 (m, 6H), 7.66 (q, 2H), 7.75 (d, 1H). GC-MS:  $m/z$  179.





p-Terphenyl(h).  $^1\text{H}$  NMR (300 MHz,  $\text{CDCl}_3$ ):  $\delta$  = 7.34-7.39 (m, 2H), 7.44-7.49 (m, 4H), 7.63-7.68 (m, 8H)

This information comes from: Sun, CL., Li, H., Yu, DG. *et al.* An efficient organocatalytic method for constructing biaryls through aromatic C–H activation. *Nature Chem* **2**, 1044–1049 (2010).



## List of Figures

<i>Figure 1. World chemical sales by region in 2017</i> .....	2
<i>Figure 2. A: new chemicals strategy that sets a long-term vision for EU chemicals policy; B: European Green Deal</i> .....	3
<i>Figure 3. Cellulose molecular structure</i> .....	5
<i>Figure 4. Variety of cellulose sources</i> .....	6
<i>Figure 5. Cellulose hierarchical architecture</i> .....	8
<i>Figure 6. TEMPO-mediated oxidation of cellulose to form C6-carboxylate groups via C6-aldehyde groups</i> .....	9
<i>Figure 7. Oxidation of primary hydroxyls to carboxyls by the TEMPO/NaClO/NaClO<sub>2</sub> system under weakly acidic or neutral condition</i> .....	11
<i>Figure 8. Production scheme of cellulose nanosponges (CNS)</i> .....	13
<i>Figure 9. Basic mechanism scheme of Suzuki-Miyaura coupling</i> .....	15
<i>Figure 10. Different Pd catalysts, A: Pd/C; B: Pd/Al<sub>2</sub>O<sub>3</sub></i> .....	19
<i>Figure 11. TEMPO-oxidized cellulose nanofibers from cotton linters</i> .....	33
<i>Figure 12. Water suspension of sonicated TOCNF (A), mixture of TOCNF, bPEI and citric acid (B)</i> .....	34
<i>Figure 13. Comparison of CNS morphology prepared with different TOCNF: bPEI ratio, for 1:2 (left) and 1:1 (right)</i> .....	35
<i>Figure 14. CNS (A) and CNS-Pd (B)</i> .....	36
<i>Figure 15. Color change of palladium chloride solution before (A) and after (B) absorption</i> ...	36
<i>Figure 16. SEM images of CNS-Pd: 10 μm and 2 μm</i> .....	37
<i>Figure 17. EDS image of CNS-Pd</i> .....	38

<i>Figure 18. EDS absorption spectrum of CNS-Pd</i> .....	38
<i>Figure 19. Distribution map of different elements of CNS-Pd</i> .....	39

## List of Tables

Table 1. Pd loading concentration on CNS-Pd.....	40
Table 2. Pd concentration on Leaching test .....	40
Table 3. Reaction result for different time and temperature.....	44
Table 4. Reaction result for different catalyst percentage .....	46
Table 5. Reaction result under the influence of base existence.....	47
Table 6. Reaction result for different TBAB percentage.....	48
Table 7. Catalysts recovery rate for reuse .....	49
Table 8. Yield result for reuse in four times .....	50
Table 9. Reactions with different substituents .....	51



## Acknowledgements

Writing here, I have mixed feelings. Looking back on my two years of study and life, I would like to thank myself for persevering. After going through a lot of ups and downs, I have never given up on my dream, and I have been able to put in my efforts. This experience will be of great use to me in the future.

Secondly I would like to thank Prof. Carlo Punta; Prof. Alessandro Sacchetti, Dr. Laura Riva and the friends in the lab, they helped me when I was at a loss and taught me a lot

Finally, I would like to thank my grandparents. Although they have passed away one after another, at this moment I think there is some joy and missing in my tears.





